Classification of Reach and Grasp Motions from EEG Signals using Deep Convolutional Neural Networks (CNN)

Author

HAJRAH SULTAN

Regn Number

319381

Supervisor

Dr. ASIM WARIS

DEPARTMENT OF BIO-MEDICAL ENGINEERING AND SCIENCES

SCHOOL OF MECHANICAL & MANUFACTURING ENGINEERING

NATIONAL UNIVERSITY OF SCIENCES AND TECHNOLOGY

ISLAMABAD

NOVEMBER 2022

Classification of Reach and Grasp Motions from EEG Signals using Deep Convolutional Neural Networks (CNN)

Author

HAJRAH SULTAN

Regn Number

319381

A thesis submitted in partial fulfilment of the requirements for the degree of

MS Biomedical Engineering

Thesis Supervisor:

Dr ASIM WARIS

Thesis Supervisor's Signature: _____

DEPARTMENT OF BIO-MEDICAL ENGINEERING AND SCIENCES

SCHOOL OF MECHANICAL & MANUFACTURING ENGINEERING

NATIONAL UNIVERSITY OF SCIENCES AND TECHNOLOGY

ISLAMABAD

NOVEMBER 2022

Declaration

I certify that this research work titled "*Classification of Reach and Grasp Motions from EEG Signals using Deep Convolutional Neural Networks (CNN)"* is my own work. The work has not been presented elsewhere for assessment. The material that has been used from other sources it has been properly acknowledged/referred.

Signature of Student

Hajrah Sultan

2019-NUST-Ms-BME-000319381

Copyright Statement

- Copyright in text of this thesis rests with the student author. Copies (by any process) either in full, or of extracts, may be made only in accordance with instructions given by the author and lodged in the Library of NUST School of Mechanical & Manufacturing Engineering (SMME). Details may be obtained by the Librarian. This page must form part of any such copies made. Further copies (by any process) may not be made without the permission (in writing) of the author.
- The ownership of any intellectual property rights which may be described in this thesis is vested in NUST School of Mechanical & Manufacturing Engineering, subject to any prior agreement to the contrary, and may not be made available for use by third parties without the written permission of the SMME, which will prescribe the terms and conditions of any such agreement.
- Further information on the conditions under which disclosures and exploitation may take place is available from the Library of NUST School of Mechanical & Manufacturing Engineering, Islamabad.

Acknowledgements

I am thankful to my Creator Allah Subhana-Watala to have guided me throughout this work at every step and for every new thought which You setup in my mind to improve it. Indeed I could have done nothing without Your priceless help and guidance. Whosoever helped me throughout the course of my thesis, whether my parents or any other individual was Your will, so indeed none be worthy of praise but You.

I am profusely thankful to my beloved parents who raised me when I was not capable of walking and continued to support me throughout in every department of my life.

I would also like to express special thanks to my supervisor Dr Asim waris for his help throughout my thesis and also for Biomedical Instrumentations and Biomedical Signal processing courses which he has taught me. I can safely say that I haven't learned any other engineering subject in such depth than the ones which he has taught.

I would also like to pay special thanks to Dr Imran Khan Niazi for his tremendous support and cooperation. Each time I got stuck in something; he came up with a solution. Without his help, I wouldn’t have been able to complete my thesis. I appreciate his patience and guidance throughout the whole thesis.

Finally, I would like to express my gratitude to all the individuals who have rendered valuable assistance to my study.

Dedicated to my father, Sultan, to my mother, Saba, to my Grandparents and to my adored Siblings whose tremendous support and cooperation led me to this wonderful accomplishment.

Abstract

Classification of neural correlates of hand motions from EEG signals recently gained attention of researchers for the development of BCI systems for persons suffered from stroke, spinal cord injury who are not able to do voluntary movements or person with amputated arm or legs. Commonly LDA, SVM and K-NN models are used for the classification of hand motions, CNN and hybrid models are also used but most methods include the complex methods or pre-processing of EEG data and extraction of time or frequency domain features from the pre-processed signals which is a time consuming and lack flexibility because the EEG signals vary from human to human. In this thesis a Deep CNN model for end-to-end learning of neural corelates for reach and grasp actions is introduced, aiming to increase rate of recognition & balanced classification accuracy throughout all the subjects. A new model of CNN for movement classification is proposed that can also be used on the edge devices because of its smaller size for the development of BCI systems. In the proposed model separable convolutional blocks are used which reduce the number of parameters and hence the size of model also decreases. The dataset that is used for the testing of model is BNCI Horizon 2020 Reach and Grasp action dataset that is publicly available dataset. The dataset is also tested on 3 machine learning models LDA, SVM and K-NN are used, in which input is given in the form of time domain feature set the average accuracies achieved on these models are 60.77 (±3.80 STD), 66.73 (±2.86 STD), and 79.81 (±3.11 STD) respectively on the unseen dataset. Then the dataset is tasted on proposed Deep learning model along with DeepConvNet and EffNet models. The proposed model achieves the average classification accuracy of 92.44 (±4.13 STD), 92.9 (±4.23 STD) and 81.7(±5.68 STD). The model proposed achieves the same accuracy as DeepConvNet, but the size of proposed model is far smaller than the DeepConvNet model. Results shows that the proposed model shows the improved results with less variation of results within the subjects. Which will become helpful in the creation of real time BCI systems.

Key Words: *EEG, Reach and Grasp, Deep Learning, Machine Learning, CNN, BCI system*

Table of Contents

List of Figures

List of Tables

List of Abbreviations

ANN	**Artificial Neural Network**
BCI	**Brain Computer Interfacing**
CNN	**Convolutional Neural Network**
DL	**Deep Learning**
EEG	**Electroencephalograph**
fMRI	**functional Magnetic resonance Imaging**
ICA	**Independent Component Analysis**
LDA	**Linear Discriminant Analysis**
MRI	**Magnetic Resonance Imaging**
MRCPs	**Movement Related Cortical Potentials**
PCA	**Principal Component Analysis**
SCI	**Spinal Cord Injury**
SVM	**Support Vector Machine**
AP	**Action Potential**
RP	**Resting Potential**
TP	**Threshold potential**
RF	**Random Forest**
MeA	**Micro electrode Array**

CHAPTER 1: INTRODUCTION

1.1 Brain-Computer Interfaces (BCI)

As present assistive technology has evolved from simple and stiff items that are designed to solely support the user's weight to advance mechatronic devices that are capable of intricate motion and mechanical support, the need for enhanced user control devices has been increasing day by day. The hardware that is being used is already sufficiently advanced enough. Now researchers have shifted their focus towards the technologies that allow humans to build a communication path between the devices more easily and control or modify the behavior. From these methods, one of the foremost techniques that build these communication paths between humans and the assistive device is Brain-Computer Interfacing or BCI systems. In the BCI system, a specific type of exocortex device is used that builds up the communication path between the human brain and the output device using the brain signals [1]. Exocortex is an implantable or wearable device that is used for enhancing the brain's cognitive actions of high-level and sending information about users' actions and decisions for example in the case of a severe spinal cord damage (SCI), regaining fundamental motor ability to grasping activities becomes challenging, BCI system is one of the possible way to regain the basic motor abilities by creates a communication link between the brain impulses and the external equipment, which may include robotic limbs, computers, or any other electronic devices. The commands and messages that are transmitted using the BCI system are encoded to the cerebral activity of the user. BCI systems are generally classified into two types first one is invasive BCI systems in which the neural activity is measured by using EEG electrodes inserted into the brain using surgical procedures. The second one is Non-Invasive BCI systems in which the brain's neural activity is measured by placing the electrodes outside the scalp or head or using other imaging methods like Magnetic resonance imaging (MRI) or fMRI for measuring the neural activity. The mostly used non-invasive method is Electroencephalography (EEG) which measures the electrical activity generated by the neurons from the scalp. The performance of movement action mentally without involving the movements of limbs or imagination of movement is known as Motor Imagery (MI). The imagination of motion generates the same neural activity rhythms in the motor cortex of the brain as the real performance of movement generates [2]. The MI-based

BCI systems, that are, the motor action imagination without the real limb movement, have a strong practical importance in the field of mobility rehabilitation (MR) & neurological rehabilitation (NR) of stroke or Spinal cord Injury (SCI) patients [3]. MR is a type of physical rehabilitation that is used by patients who are suffering from motor abilities issues, MR is used for restoring their lost motor abilities and recovering their normal level of motor abilities or helping them to learn about their disabilities. In the BCI system based on Motor Imagery, the movements can be identified by placing the EEG electrodes in the proper location over the motor cortex region of the brain [4]. The EEG signals are non-stationary, non-linear, and weak because while measuring the neural activity from the motor cortex area the EEG signals got contaminated with multiple artifact signals that are not part of the cerebral activity of brain-like, eye blink artifacts, line noises, or muscle movement artifacts. These artifacts decrease the motion detection accuracy of the system in Motor Imagery based BCI systems. So, for increasing the accuracy of BCI systems multiple techniques of artifact removal, feature extraction, feature selection, and classifications are used for the successful implementation of accurate and efficient BCI systems.

1.2 Thesis Motivation and Scope

BCI systems build an alternate communication path between a human brain and some external assistive devices. The process of motion recognition from neural correlates starts with the recording of neural activity from the motor cortex using the non-invasive EEG electrodes and continues through the pre-processing of recorded EEG signals to the identification or detection of a person's intentions. After the detection of user intention, the signal is then sent to the external output device which may be a robotic limb, electronic wheelchair, or VR headset, and control the device according to the detected motion signal. The field of BCI is nowadays a very flourishing domain of research where a large number of research groups from all over the world are doing research and studying new methods for its improvement. Brain-Computer Interfacing systems have been found very useful in a large number of applications for both unhealthy and healthy persons. But still, the development and design of an accurate and complete BCI system that can be used for commercial use is an unsolved query for the researchers. An accurate and efficient BCI system successfully recognizes and classifies the specific set of movement patterns from the recorded EEG signals. For the data collection of human neural activities Electroencephalograph (EEG) is the most convenient and user-friendly method because of its

space & time resolution along with the non-invasive application of data recording. Motor signals are very commonly used in the development of Brain-Computer Interface systems. As the signals generates during the motor activities are just like the motor signals in brain patterns, the identification of these signals is done using the signal processing unit in a BCI application. That's why the processing of EEG signals plays a vital role in the performance evaluation of BCI. By the time this research study started, the convolutional techniques of machine learning of signal processing and classification like PCA, ICA, LDA, SVM, etc. had been used along with that Artificial Neural Networks (ANN) also used in which mostly hand-crafted features were used as an input for the model instead of Raw signals these techniques were explored by multiple studies & these techniques shows efficient results under the specific conditions. However, this trend is changing, and the use of Deep Learning (DL), particularly Convolutional Neural Networks (CNN), for the classification motor signals of different hand motions from raw EEG motor cortex signals is becoming more common because these are very effective in detecting complicated features and patterns from raw time series data. Through numerous layers of neurons, the deep network may intrinsically model complex properties and non-linear interactions between these features as the neural activity of the brain in EEG signals is highly complex and non-linear activities so, the deep learning models will become more helpful in the classification & understanding of these patterns. Along with that, the continuous recording of EEG data in BCI systems generates a large size of dataset that is vital in deep network training. These factors motivated me to use the DL techniques in this study for classification aspects of the BCI system.

This study investigates BCI systems, including EEG as the signal collection technique. The primary goal of this research is to investigate the factor of signal processing factor of the BCI system. For controlling a brain-computer interfacing system, a signal from the motor cortex area of the brain is used in this research. Different machine learning methods are investigated along with that a Deep learning model is also developed that recognizes the hand movement patterns from EEG signals. The pre-Recorded publicly available dataset is used in this study, signal processing and classification part of the BCI system are studied in this research by using multiple Machine and Deep Learning techniques.

1.3 Literature Review

Traditionally neural networks were used in the early studies to classify motor cortex EEG signals in which the hand-crafted features or Wavelet Transform (WT) images are used as an input for the classification of motor signals from EEG recordings in which most data loss while manual selection of features or conversion of data into images and topo-maps to aid CNN models that prefer 2D inputs instead of using raw time series signal [5]–[10]. For the feature extraction CSP, Fourier transform, & discrete wavelet transform (DWT) are found to be the most used techniques of feature extraction and classifying motor activity EEGs in this case. In the classification of EEG signals, traditional neural networks such as LDA, SVM, Random Forest (RF), K-NN, Multi-Layer Perceptron (MLP) and CNN have been preferred as classifiers []. Table no. 1.1 are showing the compression of classification results from different classifiers and the dataset that they used for the classification purposes. [11] uses the CNN model for the classification of hand motions in which they used the self-recorded dataset (5 subjects), the classification accuracy of right-hand and left-hand motions achieved in this study is 84.61 ± 0.77% the input shape used is Channels x Time points. But for the classification of motions of same hand the [12] uses the Regularized LDA+ CSP techniques and achieves the accuracy of 56.38%. [13] Uses the same dataset that is used in this study and classifies the palmar and lateral grasp motion by using the ensembled K-NN classifier and applied the techniques of Principle Component Analysis (PCA) for the feature reduction, the average classification accuracy achieved by this study is 85.13%. [14] uses the Fast Fourier Transform (FFT), CWT coefficients and scalogram images are used for feature extraction and then the ML classifiers logistic regression, k-NN and RF methods are applied for the classification of hand motion from the extracted feature set and deep learning models also applied and highest accuracy achieved is 88%. [15] uses the hybrid approach for the classification in which they used both temporal and frequency domain information for classifying the hand opening and closing movements the model with both time and frequency domain approaches archives the classification accuracy of 76.21 ±3.77%. [16] used the hybrid DL model in which they use CNN + LSTM model for the classification of hand motion and achieves accuracy of 87.68%. But for the development of a model that can be used in edge devices the use of hand-crafted features is not a feasible solution so instead of using ML models deep Learning models should be used for the classification of

different hand motions from same hand. Table no 1.1 shows the compression of different techniques used for the classification of hand motions.

Table 1:1 Comparison of Different Studies on the Classification of hand motions from EEG signals

Ref	***Subjects***	***Electrodes***	***Type of Movements***	***Classifier***	***Accuracy***
[11]	5 Subjects	64 Channels	5 hand motions	RLDA+CSP	56.38%
[13]	15 Subjects	58 channels	Reach and Grasp	PCA + Ensembled K-NN	85.13%
[14]	---	19 channels	2 hand Motions	RestNet	85%
[15]	Prerecorded Data	---	Hand opening, closing, and resting	CNN	76.21%
[16]	Prerecorded data	22 channels	Left hand, right hand, feet, tongue	LSTM+CNN	87.68%
[17]	109 BC12000	64 Channels	Right- and Left-hand movements	ANN	68%
[18]	13 Subjects	64 EEG Channels	6 Lower Limb Movement	Random Forest with 512 trees	
[19]	9 Subjects	64 EEG Channels	6 Lower Limb Movement Tasks	K-NN SVM LDA	54%
[20]	12 Subjects	32 channels	Opening and closing of figure	ANN	79.92%
[21]	Pre-Recorded Dataset	---	Left- and Right-hand movement	LDA QDA, KNN SVM	SVM 82.14%
[22]	11 Subjects	14 Channels	Right- and left-hand movement	LDA	73.2%
[23]	2 pre-recorded datasets	---	Hand opening, closing, and resting	CNN + Spatial filtering	83.61%

1.4 Contributions of Research

The objective of this research is to develop a new proposed Deep Learning-based model that can categorize two separate motor imagery tasks: reach and grasp motions of the same hand by using raw EEG time series data. As mentioned earlier that in some previous studies on EEG motor signal classification, the EEG signals were first converted into images and topo-maps to aid CNN models that prefer 2D inputs [5]–[10] Though, this conversion of data may result in the loss of critical features & information. Because the study indicates that EEG data is connected with time, that's why raw EEG data is used in this research & seeks to learn general features. Several researchers recorded the neural activity from the surface of the skull and then converted these signals into topographical time series images [5]–[10]. But there is proof that the recorded EEG signals are connected across the time scale, implying temporal modulation [24]. CNN models have recently achieved high accuracies with 2D input EEG data i.e., TxC (Time sample x Channels) [25], [26]. For these reasons, in this work 2D, raw EEG data is used as an input shape for the CNN model but before that data is minimally preprocessed using basic bandpass and noise removal filters. Then the performance of the proposed model is compared with the well-established models like SVM, LDA, and K-NN techniques along with the different Deep learning models like "DeepConvNet", "EffNet" etc. that are developed for edge device perspective for the development of multiple applications and compare the classification results along with model sizes.

The model proposed in this research for the classification of EEG signals is efficient, uses less computational power, and is smaller in size as compared to other DL models that are previously been used for the classification of Reach and Grasp actions of the same hand. This will help in the development of real-time BCI systems on embedded devices for the development of neurorehabilitation BCI systems for Stroke and SCI patients who lose their motor abilities.

1.5 Thesis Organization

The rest of thesis is divided as follows. Chapter 2 describes the basics of BCI & how the neural activity of a person is used for operating a BCI device. The following section describes the oscillatory nature of the electrical activity of neurons & their frequency ranges. It is followed by an explanation of the causes of artifacts in EEG data and the filtration technique.

The approach used in this study is described in Chapter 3. First, a description of the dataset is provided, followed by an explanation of the pre-processing techniques used to remove undesired noise and artifacts. Finally, the techniques for feature extraction and classification that were used in this research are discussed.

Chapter 4 describes the results of this research. The EEG signals for reach and grasp motion are described first then the muscle artifacts, line noises, and eye blink components are identified from the recorded EEG data and then the removal of these artifacts from the EEG data is described by using multiple data pre-processing methods. Then next for machine learning methods feature extraction is described in which time domain features are discussed. For the DL CNN model, the raw data is used instead of hand-crafted features. Finally, the Movement Related Cortical Potentials (MRCPs) and classification results by using 3 ML classifiers and DL models are presented.

Chapter 5 summarizes the key elements of the current work. The chapter concludes with a description of the scope of future work expansions.

CHAPTER 2: OVERVIEW OF BRAIN-COMPUTER INTERFACE SYSTEM & MOTOR SIGNAL CLASSIFCATION

The objective of this thesis is to create a model that can classify distinct kinds of electroencephalography (EEG) motions to aid in the treatment & diagnosis of neurological disorders. This chapter mainly provides an overview of Human brain anatomy and physiology and the about also describes the concept of the BCI system's structure and commonly used methods for neural activity recording methods to have a broad understanding of BCI systems and the Structure and functioning of the brain, neural activity recording methods.

2.1 Introduction

The brain, as a human organ, has the unique capacity to self-adapt and generate new neuronal associations while absorbing and learning new information. The brain never stays the same. It grows and evolves over a person's life. Even as you read this sentence, fresh information is being absorbed in breakneck speed, with some of it being retained in short or long-term memory. The brain's enormous memory capacity acts as a repository for information and experience. Environmental sensing and motoric acts are also the coordination and responsibility of several brain areas. Each area is in charge of a distinct bodily part control, sensing, or mental function. However, the specific process of the brain's functioning is yet unexplained. More sophisticated brain operations, such as the conception of an idea, remain a mystery. It is impossible to map or develop a model of the brain without understanding its inner workings.

The brain has been studied by several neurophysiologists & neuroscientists who undertake studies to discover the fundamental building blocks and scientific ideas behind the behavior and structure and of the brain. By confirming and demonstrating (or disproving) one theory at a time, the whole picture is becoming clearer. There are several issues that hinder a deeper investigation of the brain. Much of the difficulty stems from the brain's unpredictability. Although every person has the same organ of the brain, it is nonetheless unique in many functional and anatomical properties. However, the new issues and limitations do not deter people from studying brain function. Many science fiction films inspire scientists to bring fiction into the real world. Only by inventing and using new methods for analyzing brain anatomy and behavior can the mysteries of the brain be revealed.

2.2 Human Brain

The brain is the supreme commander of the human body. It is the central nervous system component that regulates the operations of many organs in the body. To begin, we will discuss the anatomical structures of the brain and their activities in this part. Then complete understanding of the why, and where the brain produces these electrical impulses and how this electrical activity can be recorded from the scalp of the human brain. It gives a clear concept of the formation of electrical current flow in the brain that may be recorded by using the EEG electrodes.

2.2.1 Structure and Function of Brain

As seen in Figure no. 2.1 the brain is split into three primary parts: the cerebrum, the cerebellum, and the brainstem [27]. The three brain areas are explained briefly below.

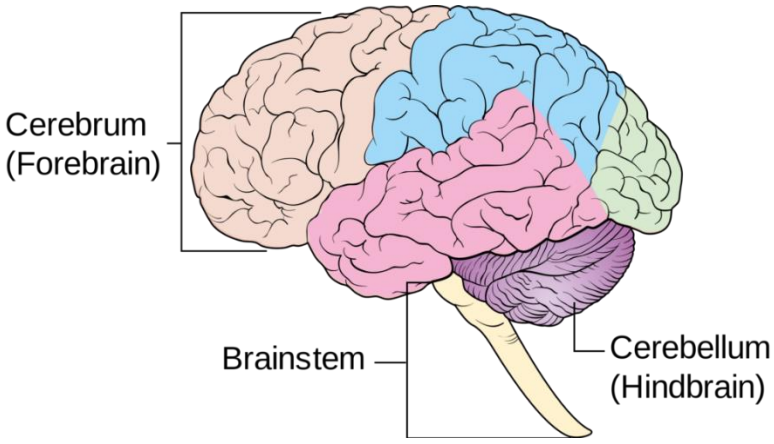

Figure 2-1 Human Brain's Anatomical Areas [28]

1. **Cerebellum:**

   The cerebellum is split into two hemispheres & is positioned in the bottom back of the skull Figure no. 2.2 shows the structure of cerebellum. It is the brain's second biggest structure, containing more than half of all neurons. The cerebellum is one of the brain's sensory centers, important for sensory perception, motor control, & coordination.

   The cerebellum is also linked to fine motor abilities, voluntary movements of muscles, balance control, & posture.

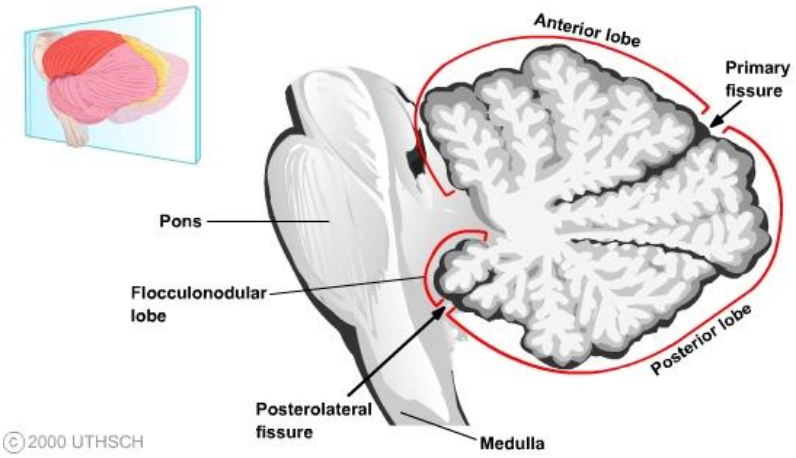

Figure 2-2 Cerebellum's Midsagittal cross-sectional area that shows the 3 primary lobes. [29]

2. **Cerebrum:**

The cerebrum is the most important & largest region of the human brain, & it is involved with brain processes such as motor skills, emotions, movements, & thoughts. The cerebral cortex is the outermost layer of the cerebrum made up of neural tissues. The cerebrum is divided into 2 halves, known as the left & right hemispheres. Each hemisphere has 4 lobes figure 2.3 shows the lobes cerebrum:

I. **Frontal Lobe:** Frontal lobe plays role in problem solving, parts of speech, Personality, motor development, planning, emotions, thinking, & movement are all influenced by the frontal lobe.

II. **Temporal Lobe:** The Temporal Lobe plays a role in speech, auditory stimuli identification, perception, & memory.

III. **Occipital Lobe:** The Occipital Lobe oversees visual processing.

IV. **Parietal Lobe:** The Parietal Lobe oversees feeling (e.g., touch, pain etc.), sensory recognition, understanding, direction, stimulus perception, & movement.

3. **Brainstem:**

The brainstem connects the cerebrum to the spinal cord and is positioned at the bottom of the brain figure no. 2.4 shows the structure of brain stem. The brainstem functions as the body's main control panel, much like a computer's hard drive. It regulates critical bodily

processes such as awareness, breathing, mouth & eye movements, & the relaying of sensory messages (heat, pain, noise, and so on), blood pressure, heartbeat, & hunger.

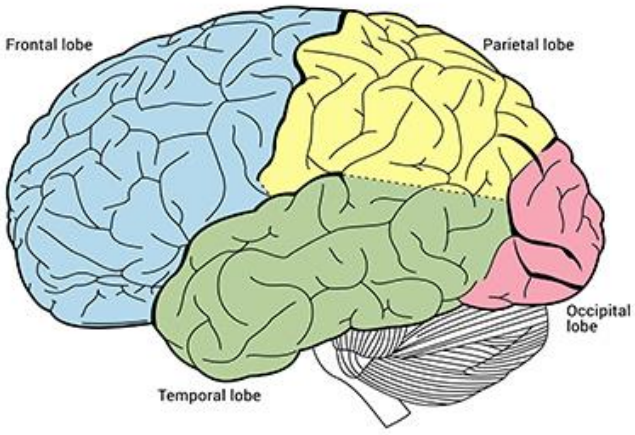

Figure 2-3 4 Lobes of Human Brain [30]

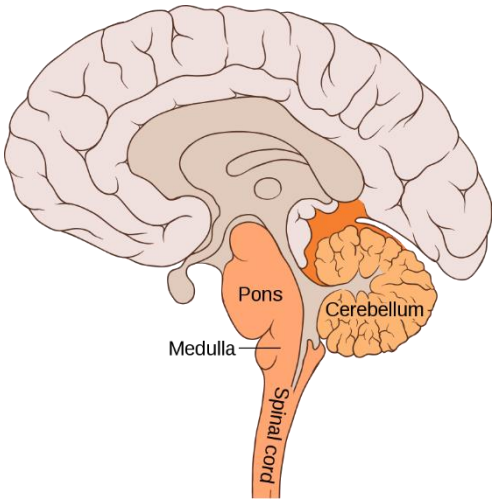

Figure 2-4 Human brain's sagittal section showing 3 main parts of the brainstem. [31]

2.2.2 Neurophysiology of the Human Brain

The human brain is made up of around 100 billion nerve cells known as neurons, which maintain the brain's electrical charge [32]. Neurons contain the same components and properties as other cells, but their electrochemical nature allows them to conduct electrical messages and impulses across great distances. Neurons are made up of three fundamental components:

I. Dendrites

II. Soma (the cell body)

III. Axon

Figure no. 2.5 shows the basic structure of neuron.

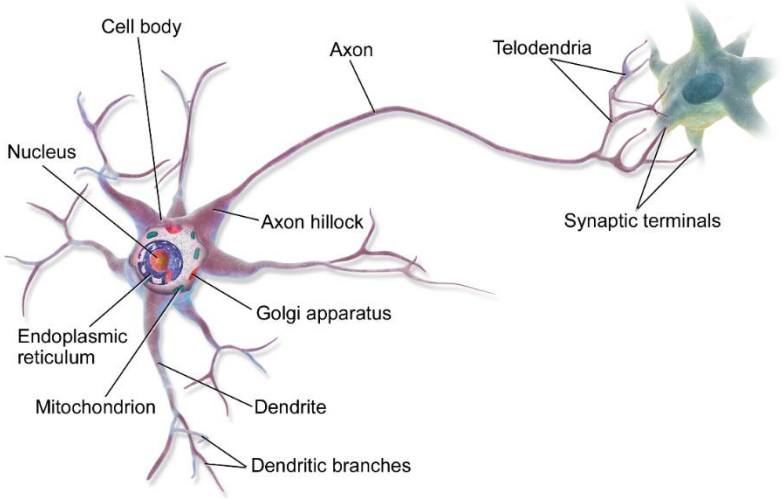

Figure 2-5 Structure of Neuron [32]

The cell nucleus is the cell's heart, giving it guidance regarding what to do. The axon is a thin and long part of a neuron that links its own nuclei to the dendrite of another neuron. The dendrite is a small portion of the neuron that contains several sites that act as receptors for neurotransmitters delivered by a linked axon. Dendrites can grow on either one or both ends of the cell. Neurons can interact with one another via the axon dendrite link. Neurons send and receive impulses in a predictable sequence. This connection is enabled by the Action-Potential (AP). Firstly, the resting potential (RP) is a negative electrical potential across the cell membrane of the neuron while it is at rest. Then the membrane potential increases when the neuron is triggered by electrical inputs from other neurons. If the membrane potential exceeds a specific threshold, it will rapidly grow to a substantially higher value before swiftly decreasing & stabilizing at the resting potential. When an AP fires in a neuron, it is transmitted up the axon to related neurons, where it may cause an AP to fire in those neurons as well. That's how data is transmitted & processed in biological brain networks. It's worth noting that the AP is an all-or-nothing response means either it fires, or no data is transmitted from the axon. Thus, rather than the intensity of electrical impulses, information in the brain is represented by the frequency of AP's. Figure no. 2.6 shows the graphical representation of action potential.

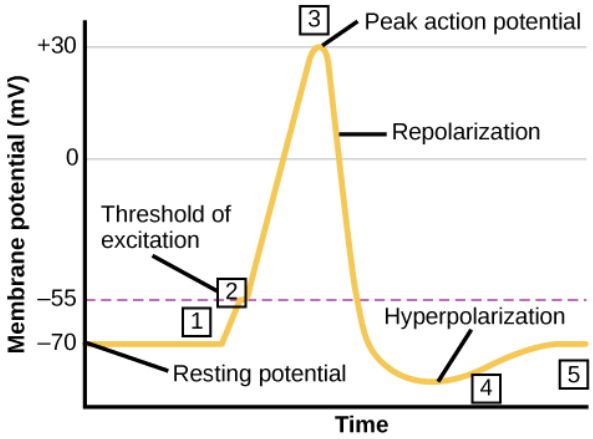

Figure 2-6 Action Potential [33]

Ion channels open's when neurotransmitter particles attach to receptors on a neuron's dendrites. This hole allows positive ions to enter the neuron, resulting in membrane depolarization, a reduction in the differential in voltage between the interior & outside of the neuron [33]. A sensory cell or another neuron's stimulation depolarizes the target neuron to 55mV Potential known as threshold potential (TP). The axon hillock's Na+ channels open, allowing positive ions to enter the cell. When the sodium channels open, the neuron depolarizes entirely to a membrane potential of roughly +40 mV. After depolarization, the cell must "reset" its membrane voltage to its RP. To do so, the Na^+-channels shut & cannot be opened. This begins the neuron's refractory phase, during which it is unable to generate another AP because its sodium channels are closed. Simultaneously, voltage-gated K^+-channels then open, enabling K^+ to exit the environment of cell. As K^+ ions exit the cell, the membrane potential returns to a negative state.

Post-synaptic Potentials (PSPs) are another source of electrical activity in the brain. These are variations in membrane potential induced by substances binding to neuron receptors. Depending on the kind of receptor bound, the RP of membrane may rise or depolarize in the case of Excitatory-postsynaptic potentials (EPSPs) decrease or hyperpolarize in the case of inhibitory post-synaptic potentials (IPSPs). In the event of an EPSP, the membrane potential is pushed closer to the AP threshold, increasing the likelihood of firing. An IPSP has the reverse effect, lowering the likelihood of the AP activating. This is how hormones, neurotransmitters, psychotropic chemicals, & other substances interact with the neurological system [34].

The sum of a large group of neurons' electrical activity has a detectable influence on the electromagnetic environment that surrounds the head. Every neuron does not contribute equally to the field measured by EEG. The neurons that contribute to EEG are mostly those that create

open fields [35]. Pyramidal neurons, a kind of neuron found in the cerebral cortex, create open fields. When these neurons fire synchronously, they produce coherent electric and magnetic fields similar to those of a dipole as shown in figure no. 2.7.

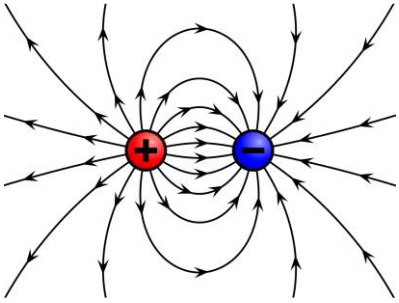

Figure 2-7 Illustration of Dipole [36]

These fields are measurable. MEG is created by measuring magnetic fields, whereas ECoG is created by monitoring electrical fields via subdermal implants. Finally, researchers record EEG by attaching electrodes on the scalp.

2.2.3 Neural Activity Measuring

Hemodynamic & Electrophysiological activities are produced by brain activity. Brain state data extraction strategies are essential to understand & analyze how the brain operates. There are several sensors that can identify various forms of neural activity. On the basis of signal acquisition techniques BCI systems are divided into two categories: invasive & non-invasive. Figure no. 2.8 shows different types of different types of Brain signals recording methods & Table 2.1 represents the comparison of these methods several signal collection methods.

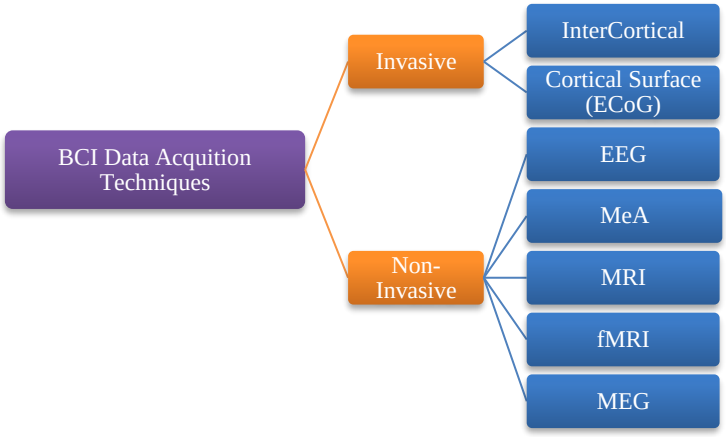

Figure 2-8 Methods of data recording for BCI system

Table 2:1 Different Methods for Brain Signals Recordings

DATA ACQUISITION TECHNIQUES	*MEASURED NEURAL ACTIVITY*	*INVASIVE/NON-INVASIVE*	*PORTABILITY*	*INDIRECT/DIRECT DATA MEASUREMENT*
EEG	Electrical	Non-Invasive	Portable	Direct
MEG	Magnetic	Non-Invasive	Non-Portable	Indirect
MRI	Magnetic	Non-Invasive	Non-Portable	Indirect
FMRI	Magnetic	Non-Invasive	Non-Portable	Indirect
ECOG	Electrical	Invasive	Portable	Direct
MEA	Electrical	Invasive	Portable	Direct

Magnetic Resonance Imaging (MRI) and functional Magnetic resonance imaging (fMRI) is one of the procedures utilized for brain scanning. This approach identifies variations in blood flow in active brain areas. It is generally recognized that blood flow rises in more active areas of the brain. This brain mapping approach has been the most widely employed since fMRI equipment were accessible in the early 1990s. It also gained popularity because it does not necessitate any additional medical intervention like surgery or the ingesting of radioactive material. The primary disadvantages of this technology are the non-real-time data recording and long scan times performance. However, innovative strategies for improving and temporal & spatial resolution are also being investigated. As in the invasive approaches sensors that are used need to place within the brain for recording brain impulses. Because they are placed into the brain, micro-electrode arrays (MeA) are very invasive. Electrocorticographic (ECoG) activity recording is another invasive technique in which sensors are put on the brain's surface rather than inside it. Despite their capacity to capture precise signals, intrusive approaches are less suitable for BCI applications due to surgical risks and implant-related issues. However, ECoG & MeA have been employed in several research for BCI applications. Although EEG is the most utilized kind of signal in BCI, it should be emphasized that a significant and quickly rising portion of BCI research is devoted to the use of implanted electrodes that record the activity of a set of neurons [37]. Implanted electrodes enable the acquisition of data with significantly higher quality & spatial resolution than non-invasive approaches [38]. Invasive technologies may measure the activity of individual neurons, but non-invasive approaches, such as EEG, can monitor the activity of thousands of neurons in real time with minimum risk.

2.3 Electroencephalography (EEG)

EEG uses electrodes that are placed on the scalp to for measuring and recording the electrical activity generated by the brain. The total of the PSP generated by hundreds of neurons with the same radial direction with respect to the scalp is measured by EEG. Hans Berger performed the first EEG measurements on a human subject in 1924. He came up with the name electroencephalogram at that time. In 1929, his key discovery was published [39]. EEG signals have a very low amplitude of range of few microvolts. As a result, before digitizing & processing these signals, they must be amplified significantly. EEG signal measurements are often done with several electrodes ranging from 1 to around 256, with these electrodes commonly secured to use an elastic cap. The application of a conductive gel or paste improves the contact between the electrodes and the skin but the dry electrodes irrespective of the wet can be directly placed on scalp area for data recording without any conductive gel. As a result, the electrode montage method is often arduous and time-consuming. It is worth noting that BCI researchers have recently suggested and tested dry electrodes for BCI, that is, electrodes that do not require the use of conductive gels or pastes [40], [41]. However, the performance of the resultant BCI was on average 30% lower than that of a BCI based on conductive gels or pastes. In general, electrodes are positioned and identified using a common model, particularly the 10-20 international system [42]. These numbers indicate that the gap in between electrodes is 10% or 20% of the skull's front-back or right-left distance as shown in Figure no. 2.9. The 10—10 method as shown in Figure no. 2.10 is also often utilized. These systems additionally provide a terminology for specifying sensor locations. Each letter represents a different lobe of the cerebral cortex, Table 2 shows the different lobes with their symbolic representation of 10-20 system:

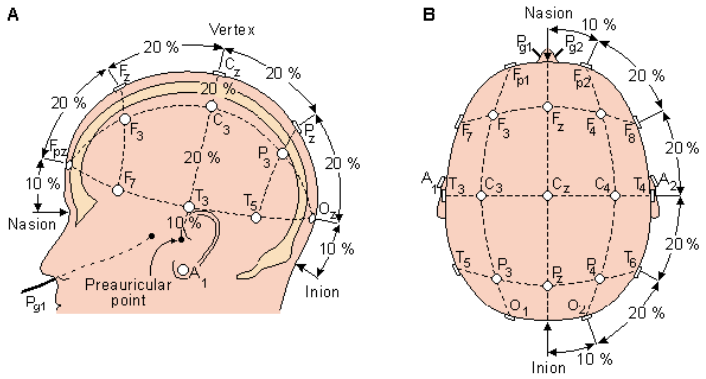

Figure 2-9 10-20 System [43]

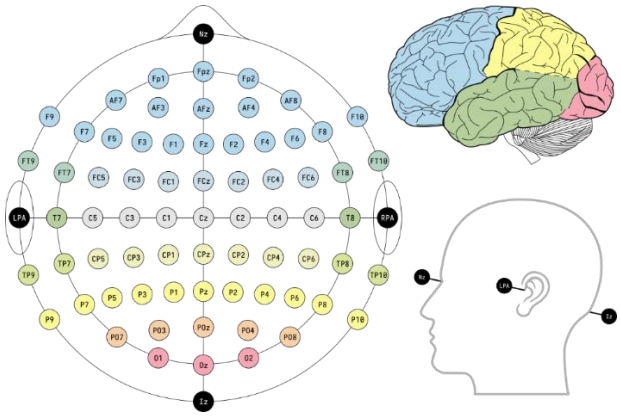

Figure 2-10 10-10 System [44]

Table 2:2 *Cerebral Cortex Lobe Division in 10-20 System*

LOBES OF CEREBRAL CORTEX	SYMBOLS
PRE-FRONTAL LOBE	Fp_z
FRONTAL	Fz
VERTEX	C_Z
OCCIPITAL	O_Z
PARIETAL	p_Z

The letter "C" does not denote a lobe, bu rather "Central." The sensors are also labelled with numbers. The electrodes along the midline of the skull are designated by the letter "z." The remaining sensors are numbered, with odd numbers to the left of the midline & even no. to the right. The "A"s denotes the ears, which are frequently used as reference electrodes.

2.3.1 Types of EEG Signals

EEG signals are made up of distinc oscillations known as rhythms [45]. These rhythms have specific spectral & spatial localization features. Figure 2. Represents the six classical brain rhythms.

I. **Alpha Waves (8-12 Hz) (α):** These are waves arise mostly in the rear regions of the brain that is occipital lobe of cortex when the subject's is in relaxing state with eyes closed.
II. **Beta Waves (13-30 Hz) (β):** This is a reasonably quick wave. These are found among awakened & mindful individuals. This rhythm is also influenced by movement performance in the motor cortex.

III. **Delta Waves (1-4 Hz.) (δ):** This is a slow wave with a relatively big amplitude that is mostly detected in adults during deep sleep.

IV. **Theta Waves (4-7 Hz.) (θ):** This is a somewhat quicker waves that is mainly detected during sleepiness and in young infants.

V. **Mu Waves (8-13 Hz.) (μ):** These are waves seen in the sensorimotor & motor cortex. When the subject moves, the amplitude of this wave changes. As a result, this wave is sometimes referred to as the sensorimotor rhythm.

VI. **Gamma Waves (30 Hz. or above) (γ):** This wave is often classified as having a maximum frequency between 80 and 100 hertz. It is linked to a variety of motor & cognitive activities.

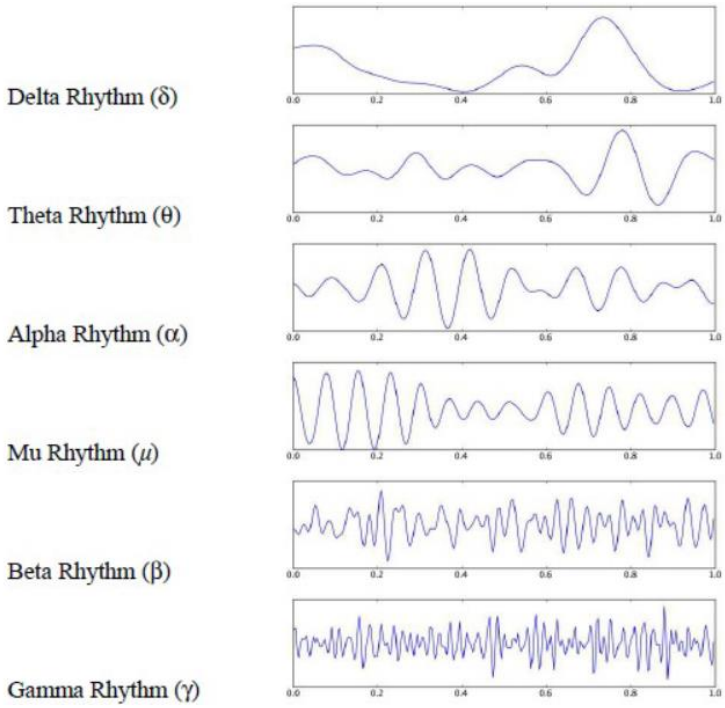

Figure 2-11 Types of Brain Waves

2.4 Brain Computer Interface (BCI) System

BCI system is defined as a "control & communication channel that does not rely on the brain's regular peripheral nerve & muscle output pathways" [46]. Commands & Messages transmitted via BCI are encoded in the user's brain activity. BCI technologies enable direct communication between the brain and a computer [46]. The goal of a BCI is to offer people with

an alternative communication channel by analyzing the brain's thought activity & permitting direct transmission of messages from the brain. A BCI is a technology that discovers a new communication means of commanding machines using just the brain. A cap with EEG electrodes is put on a user's head to measure EEG signals. To control devices, a user imagines a certain goal, such as word composition or limb movement. These tasks have an impact on the patterns of EEG signals. Computers categorize & recognize these patterns in order to operate a computer program such as movement of cursor or a machine like a brain control wheelchair.

BCIs, unlike all other interfaces, do not involve physical movement, and hence may be the only mode of communication available to those with severe motor limitations. BCIs can also be used to control & communicate other user goals & groups, such as patients with less severe motor disabilities who want to control a wheelchair or orthosis [47] & healthy users in scenarios where traditional means of communication are impractical, difficult, or insufficient [48]. BCIs may also aid in the reduction of symptoms associated with autism, stroke, & emotional and attention disorders [49]. BCIs are classified into 2 main types as discussed in section 2.2.3: invasive (based on signals collected from electrodes implanted over the cerebral cortex) & non-invasive (based on signals recorded from electrodes placed on the scalp (outside the head) [45]. According to current studies, the non-invasive EEG approach is the most desirable.

2.4.1 BCI system Architecture

A Brain Computer interfacing system typically necessitates the following closed-loop procedure, which is represented in Figure no. 2.12: brain activity monitoring, pre-processing, feature extraction & reduction, classification into different classes, translation into required output [50].

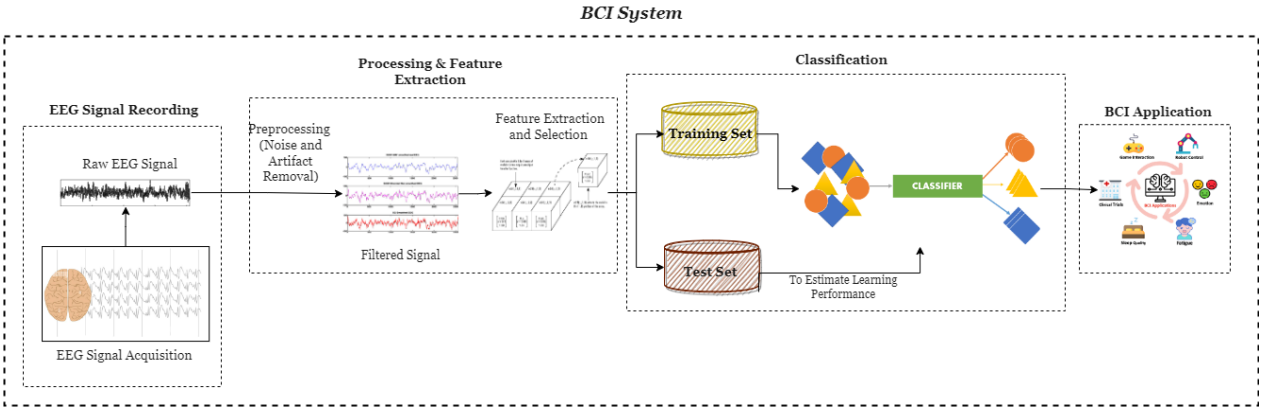

Figure 2-12 Architecture of BCI system

I. **EEG Signal Recording:**

Effectively measuring brain activity is a vital step in BCI communications. Human thoughts influence electrical impulses that are monitored using various types of electrodes and then digitized. In this thesis, EEG signals are employed to assess brain activity.

II. **Pre-Processing of EEG data:**

Pre-processing simplifies later processing procedures while enhancing signal quality without sacrificing information. The recorded signals are cleaned and denoised in this stage to increase the important information included in the signals [51].

III. **Feature Extraction:**

Certain characteristics distinguish the brain patterns employed in BCIs. The goal of feature extraction is to describe the signals using a few meaningful variables known as "features" [51].

IV. **Classification:**

Classes are assigned to a set of features derived from the signals during the classification stage. This class relates to the recognized mental states. This stage is also known as "translation of features."

V. **Application:**

Once the state of mind has been determined, a signal is connected with it in order to operate a specific application, such as a robot or a computer.

Only certain patterns of activity in continuous brain impulses linked with specific tasks or events may be detected and classified by a BCI. The mental approach employed by a BCI system determines what a BCI user must do to generate these patterns. The core of every brain computer communication is the conceptual approach. The mental approach dictates what the user must do to generate brain signals that the BCI can understand. BCIs based on selective attention, on the other hand, require external stimuli given by a BCI system. Stimuli can be either somatosensory or auditory.

2.4.2 EEG based BCI as Classification System

EEG signals are often encoded in a high-dimensional feature space, making manual analysis extremely challenging. Machine learning algorithms are useful for deciphering high-dimensional

feature sets and analyzing brain signal pattern properties. According to [] there are 5 types of classifiers utilized in BCI research. Nonlinear, linear, neural networks, closest neighbor, & a mix of these are examples of classifiers. Linear classifiers are discriminant algorithms that discriminate between classes by using linear functions. These are the most often used techniques in applications of BCI. In BCI research, neural networks are also often employed classifiers. A neural network is a collection of artificial neurons that may generate nonlinear decision limits. Nonlinear classifiers generate nonlinear decision boundaries, allowing for more efficient rejections of unclear data points as compared to discriminative classification techniques.

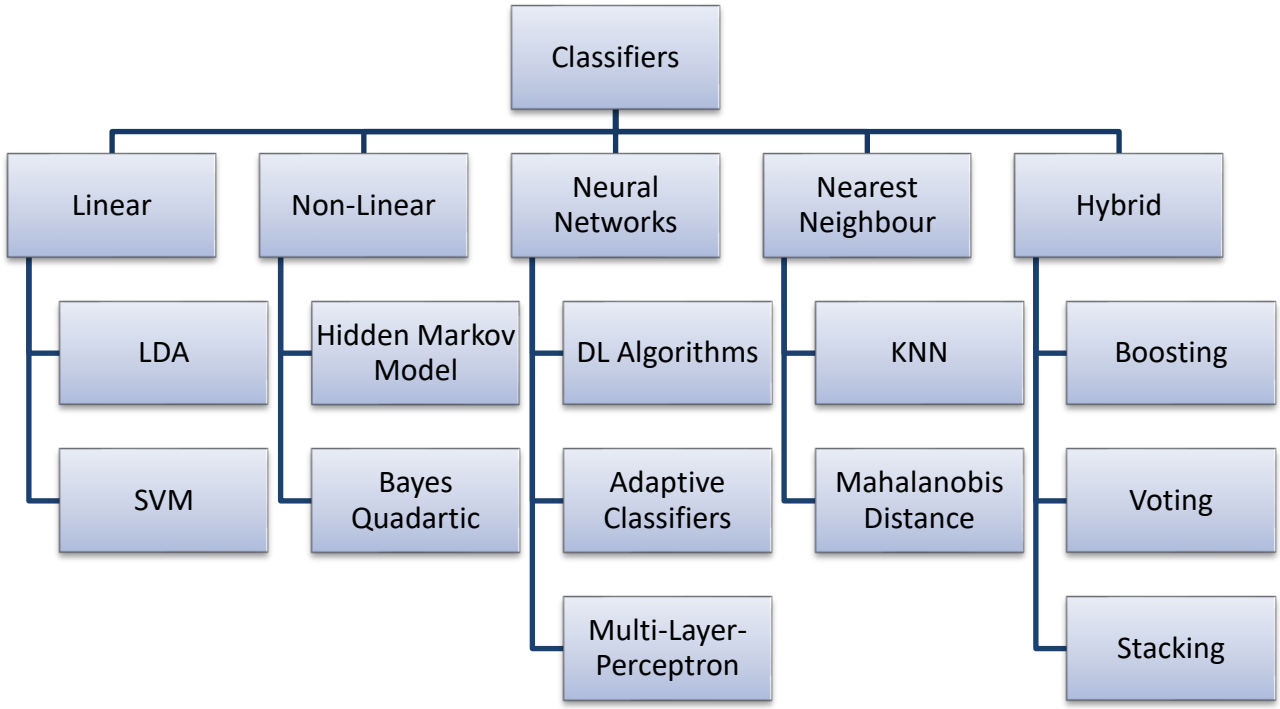

Figure 2-13 Classification Techniques used in BCI systems

2.5 Deep Neural Network (DNN)

The term "deep" has two meanings in the context of deep neural networks. The number of layers in a neural network is measured by its "depth." The second meaning comes from deep learning: machine learning algorithms that learn data representations rather than merely how to classify them. The hidden layers in an ANN are typically seen as transforming the data in a way that benefits classification. Thus, by adjusting the hidden layer's weights and biases, the network learns how to turn the input into a better representation. More complicated changes can be performed by stacking layers. DNN's were long thought to be too complicated to train to be

practical. However, in 2006, Geoffrey Hinton developed a quick training approach for a form of NN known as a “Deep belief network”, which reinvigorated DN research [52]. While [53] initially described the CNN in 1998, the continuing DL revolution began when [54] won the ImageNet Challenge with a CNN-based solution. The ImageNet competition is an annual competition in which research teams assess algorithms and compete for the highest score on picture classification tasks using the "ImageNet" labelled image dataset. [54] reduced the current error rate from 26.1% to 15.3%.

DL is a subset of ML that progressed from standard methodologies to artificial neural networks (ANN). ANNs are computer systems that were inspired by the human brain. They are made up of numerous computing units known as neurons, which conduct a fundamental operation and send the results of that action on to other neurons.

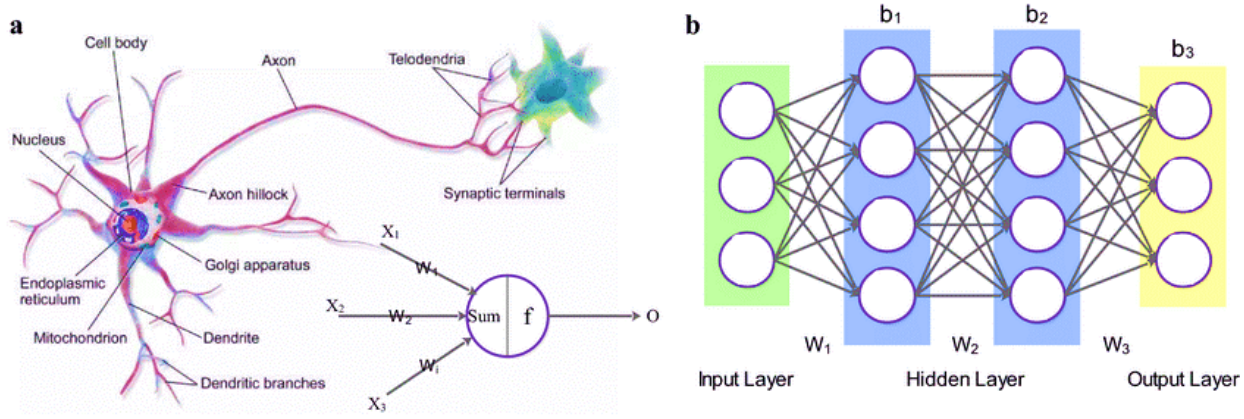

Figure 2-14 a: Biological neuron’s anatomy (Left) & b:artificial neuron structure (Right) [55]

In general, the procedure is a summation of the information received by the neuron, followed by the application of a simple, non-linear function. These neurons are subsequently grouped into units called layers in most neural networks. Although the processing of neurons in one layer often feeds into the computations of the next, certain types of networks enable information to travel within levels or even to prior layers.

2.5.1 Architecture of NN:

A NN is produced when individual neurons are connected in a network [56]. A deep layered network, or DN for short, is one that has more than 3 levels. The most typical DN design is feedforward, in which the input flows towards the output and there is no feedback link to prevent model results from being sent back into the input branches. Fig. 3.4 depicts a rudimentary

example of a feedforward neural network with L layers. There are 3 sorts of layers in a DN. The leftmost layer is referred to as the input layer, the intermediate layers as the hidden layers, and the rightmost layer as the output layer as shown in Figure no. 2.14. Since a DNN is made up of many layers, calculations are given in vector form for better comprehension and diagnosis if mistakes arise.

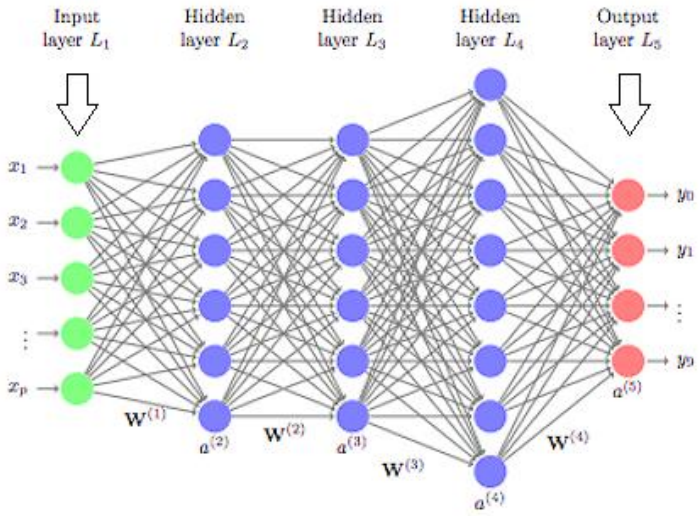

Figure 2-15 Architecture of DNN with L no. of Layers [57]

2.5.2 Convolutional Neural Network

All global patterns of the input space are learned in an CNN. For example, if the input space is a picture, the global patterns are all of the image pixels [58]. Thus, if a picture with a resolution of 32 32 is provided as an input to a layer with 1000 neurons, the total number of parameters in the network is 32x32x1000 = 1024000. (1.024 million). This is where CNNs can help. Rather than learning global patterns, CNNs learn crucial local patterns observed in the input space. Fig. 3.5 illustrates how CNN learns spatial patterns using an input picture (the number 'four') retrieved from an input dataset (MNIST).

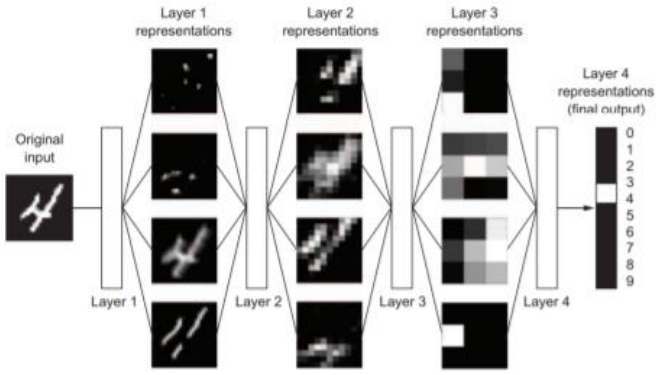

Figure 2-16 Deep Representation in Convolutional Neural Network Model [59]

A CNN model is made up of multiple layers. For simple understanding, there are 3 major layers as shown in Figure no. 2.16, in every CNN model these are:

I. Convolutional Layer (That can be 1D ,2D or 3D)

II. Pooling Layer (Max pooling, Average Pooling etc.)

III. Fully Connected Layer

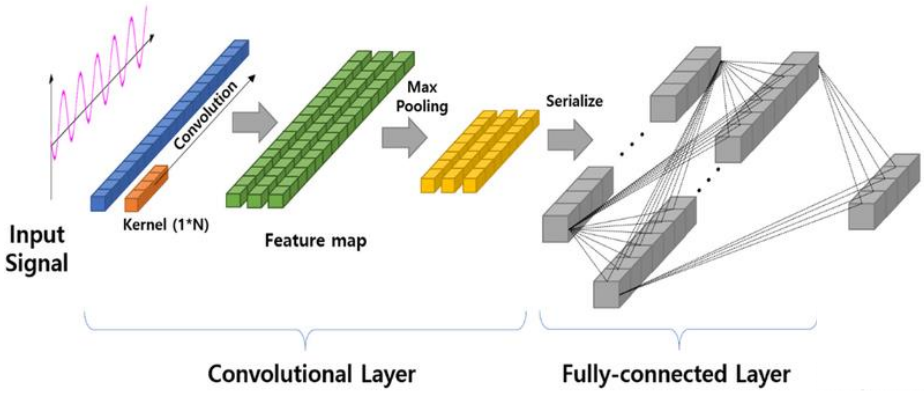

Figure 2-17 General Architecture of CNN model for Signal Patterns Classification [60]

2.5.2.1 Convolutional Layer

Conv layer is the crucial building block of any CNN. This layer performs the convolution operation between an input image and one or many kernels of the layer. Simply put, a kernel or filter is a set of weights, and the convolution operation between the image and the kernel means sliding the kernel across the image with a user-defined step size (stride) and computing the weighted sum of the small area (patch) of the image. After all the patches are generated, they are

then applied to an activation function resulting in a final output called a feature or activation map.

2.5.2.2 Pooling Layer

Another critical component of any CNN is the pool layer. To produce its output, this layer connects the output of multiple nearby elements of the activation map supplied from a preceding Convolutional layer. As a result, this process significantly decreases the number of parameters in a CNN and aids in the prevention of overfitting. Overfitting occurs when a model or classifier generalizes well to training data but not to test data.

2.5.2.3 FC (Fully Connected) Layer

The feature map from the previous Conv or Pool is flattened into a single vector of values and sent to the FC layer. A FC layer is comparable to an ANN in that it conducts the same mathematical procedure. After passing through all FC levels, the last layer of a CNN employs a problem-specific activation function to determine the likelihood that the input belongs to a certain class [61]. The SoftMax function is used as the activation function when the issue involves multi-class classification (for example, digit recognition). If the task involves binary-class classification (such as email spam detection), the activation function is the sigmoid function. Figure no. 2.17 shows how FC layers may be used for multi-class categorization.

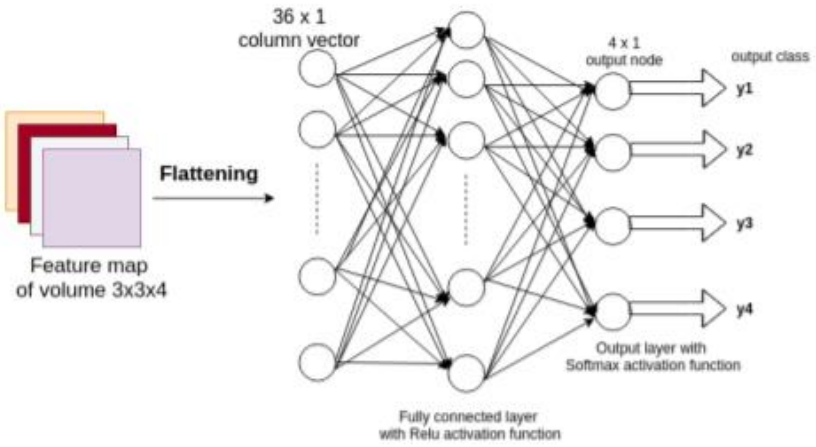

Figure 2-18 Illustration of the fully connected (FC) layers for multi-class classification [62]

CHAPTER 3: METHDOLOGY

This chapter describes about the dataset that is used in this research, details about its implementation and the structure & training of the proposed Convolutional Neural Network Model for classification of hand motions from neural corelates. In this thesis the Machine learning and deep learning both classification approaches are used on hand-crafted features set and raw signals respectively for the classification of Reach and Grasp motions.

3.1 Methods & Materials

In this research the dataset used in BNCI Horizon 2020 Reach & Grasp action decoding from Gel based EEG electrodes [63]. It is a Coordination & Support Action project that is funded in the European Commission's Framework Program 7. The aim of this project is to develop neural computer interaction devices that can help mankind with multiple perspectives.

3.1.1 Participants & Recordings

The dataset used in this research in publicly available dataset, its recording procedure was conducted by the Institute of Neural Engineering, Graze University of Technology. The dataset is recorded using the g.tec USBamp/g.tec Ladybird System that is a gel-based EEG recording system from, developed by the g.tec medical Engineering GmbH Austria, they develop both invasive & non-invasive BCI technologies that are used all over world for recording the neural activities with highest resolution. For recording the data of Reach and Grasp action they took the 15 abled right-handed persons. Before recording the data, all the participants gave the written consents forms & they also received compensation amount for participating in the experiment. From the 15 participants 5 of them were female and 10 were male with the age between 15 to 30 years. For recording the EEG data 58 active EEG electrodes were placed using the 5% grid system over the Frontal lobe, Central lobe & Parietal lobe [64]. Along with that they also used 6 Electrooculogram or EOG electrodes that were placed superior & infra orbitals on the right & left eyes and on the canthi outer side for recording the eye movement data. As a ground they used "AFz" channel and for reference they used right side earlobe. They used the 8^{th} order Chebyshev filter with the cutoff frequency range 0.01 Hz. to 100 Hz. for the prefiltering of recorded data. They set the sampling frequency on 256 Hz and apply the 50 Hz. notch filter for suppressing the power line noise that contaminate the EEG data. All the dataset they recorded

were then synchronized using the “TOBI Signal Server” [65]. For recording the movement onset time point and the time point of object grasping for each object that was used in the activity by using the “Forcesensing Resistor” (FSR) sensors. The output of the sensors was digitized with the help of Arduino that is a battery-operated microcontroller [66].

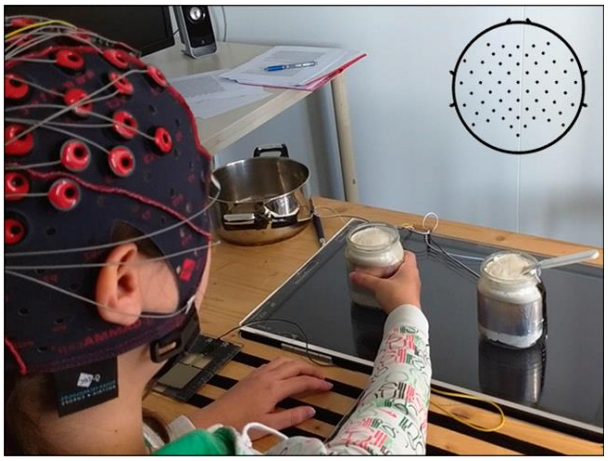

Figure 3-1 Experimental Setup of Gel-Based EEG data recording system [66].

3.2 Experimental Setup

For recording the data, the same experimental format was used as used by the [67] in his study. For recording the data for gel-based EEG electrodes the experiment was conducted in the controlled laboratory environment where the subjects were asked to sit on chair placed Infront of table with “sensorized” surface in an electromagnetically shielded room without noise. Subject was instructed to place his/her right hand on the “sensorized” surface of the table that was placed in front of them. On the table they placed a jar with spoon placed in it along with an empty jar as shown in Figure no. 3.2. Both the jars were placed on the comfortable reaching distance halfway from the right hand of the subject. Then subject was asked to perform the action of reach & grasp for both the objects one by one by using their right hand. In case of jar with the spoon the subject grasps the spoon from the by using the motion of lateral grasp & in case of empty jar the subject reach the jar and hold it by using the palmar grasp motion. The subjects were instructed to gaze the object for about 2 seconds time and then start the action of reach & grasp. Subjects performed this experiment in self-initiated way without any visual or verbal clues. Once the subjects reach the object, they were asked to hold it for 1 to 2 seconds time as shown in Figure

no. 3.3. Then finally subject returned his/her right hand back to its normal or starting position. There was a display which gives the subject information about the number of grasping action he/she had performed on the objects placed on the table that display was inserted in the surface of table. Before starting a new trail, the subject took rest of 4 seconds and then starts the next motion. In this way they recorded the data of 80 trials per condition (TPC). Totally they performed this experiment in 4 runs in each run subject perform 20 trails of each motion and after every run subject took the pause of 4 seconds before starting the next run [66]. They also recorded the data rest in which subject was instructed to focus their gaze on a fixed-point present in the center of table, they recorded the data of rest for 3 minutes at the start of 1st run after the 2nd run and then at the end of the 4th run. The data of eye movement recordings were also recorded by using the 6 EOG channels in which they recorded the vertical and horizontal eye movements by using the same method as followed by [67].

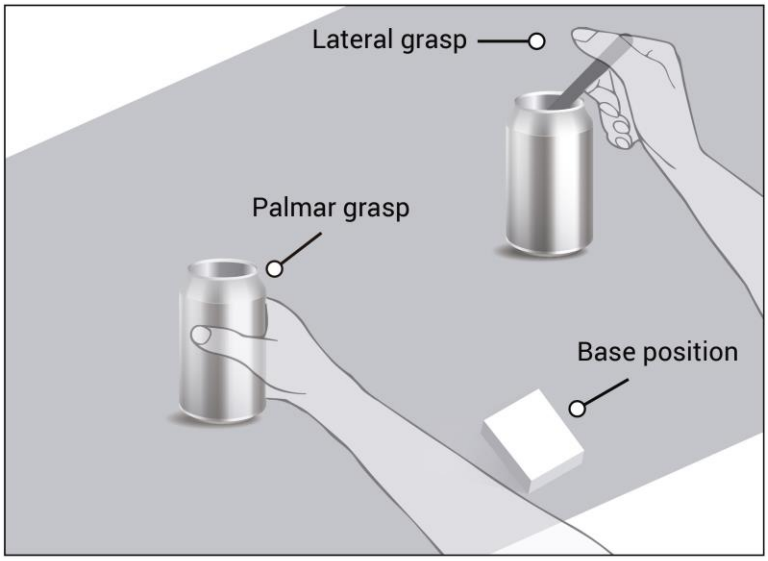

Figure 3-2 Experimental setup, object placed on table surface for Reach and Grasp (Palmar & Lateral Grasps) [66]

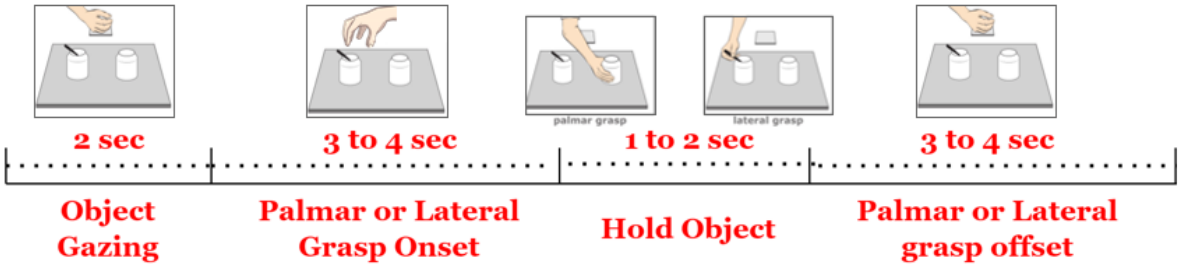

Figure 3-3 Timeline of each trail. Subject gaze object for 2 sec, the performed the motion of reach & grasp. Grasp the object for 1 to 2 seconds. Finally returned the hand back to starting position and take rest of 4 sec & start the next trail

3.3 Pre-processing of Data

The EEG data is non-stationary in nature and while recording data it contaminates with multiple artifacts like line noises, muscle activities etc. Along with that the offline re-referencing of recorded data is also required, and for that multiple referencing techniques are being used. The techniques that are followed in this study are explained in below section.

3.3.1 Common Average Referencing (CAR) Filter

Re-referencing is the process of changing the reference offline after recording. The goal of re-referencing is to express the voltage at the EEG scalp channels in relation to a new reference. It can be made up of any recorded channel or an average of several. This ultimate reference for data will have an impact on the analysis & should be chosen carefully. [68] used the CAR filter and proves that the CAR filter improves the Signal-to-Noise ratio (SNR) of EEG signal of motor and sensorimotor cortex areas that helps in extracting the motor activity from neural correlates.

The new reference when using the so-called CAR filter is the average electrical activity measured across all the EEG channels. Re-referencing is accomplished by averaging all EEG channels & then subtracts the resulting signal from each. The overall amplitude across all channels will sum to zero after re-referencing at each time point. The amplitudes will be reduced overall when using this reference, but each channel will contribute equally to the new reference. The re-referenced signal should not be biased towards any specific location on the scalp, in theory. However, electrodes are not always evenly distributed across the head. Rather, electrodes are frequently placed more densely on the top of the head, with no coverage of the underside. The amplitudes in this region will be reduced if the signal on top of the head is overrepresented in the reference. To reduce this bias, the average reference must have a high coverage of at least 64 to 128 EEG electrodes [69]. Ideally, EEG electrodes should be evenly spread out & cover up more than 50% of the surface of head [70]. [70] also encourages reporting of which channels were included in the average reference to allow for replication and comparison to other studies.

3.3.2 Butter-Worth Filter

As the raw EEG data contains a lot of artifacts there's a need to remove these artifacts and improves the SNR of signal so that required information can be extracted from EEG signals. The most efficient and commonly used technique for filtration of EEG signals is Butterworth Filter.

A Butterworth filter is a type of signal processing filter that is designed to have the flattest frequency response possible in the passband. As a result, the Butterworth filter is also referred to as a "maximally flat magnitude filter." Stephen Butterworth, a British engineer, and physicist, invented it in 1930 in his paper "On the Theory of Filter Amplifiers."

The Butterworth filter's frequency response is flat in the passband (i.e., a bandpass filter) and rolls off to zero in the stopband. The order of the filter influences the rate of slide response. The order of the filter is determined by the number of reactive elements used in the filter circuit i.e., capacitor & inductors. But in case of Butterworth filter only the capacitor is used as a reactive element and the number of capacitors define the order of the filter. In the case of the Butterworth filter, however, only capacitors are used. As a result, the order of the filter is determined by the number of capacitors. Figure 3.4 shows the circuit diagram of 4th order butter worth filter that is used in this study for filtering the EEG signals.

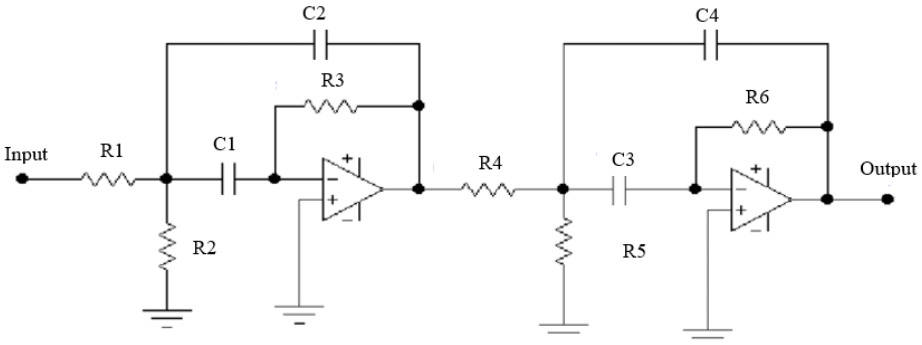

Figure 3-4 Circuit Diagram of 4th Order Butterworth Filter

The designer attempts to achieve a response that is close to the ideal filter while designing the filter. It is extremely difficult to match results to the ideal attribute. To achieve an attribute that is close to the ideal, filter with higher orders must be employ complex. The general Transfer Function (TF) of the 4th order Butterworth bandpass filter is given in equation 3.1.

$$A(s) = \frac{\frac{A_m(\Delta\Omega)^2}{b_1}.s^2}{1+\left[\left(\frac{q}{b_1}\Delta\Omega\right)s\right]+\left[\left\{2+\frac{(\Delta\Omega)^2}{b_1}\right\}s^2\right]+\left[\frac{a_1}{b_1}\Delta\Omega s^3\right]+s^4} \quad (3.1)$$

The figure no. 3.5 shows the frequency responses of the bandpass Butterworth filters of different orders.

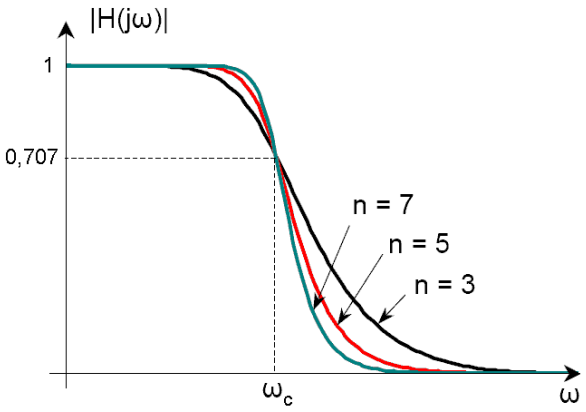

Figure 3-5 Frequency response of Butterworth Filter

Figure no. 3.6 shows the frequency response of 4th order with cutoff frequencies 0.01 to 35 Hz. that is used in this study. The filtration of EEG data is done by using the "ERPLAB" that is used for EEG data preprocessing in MATLAB®.

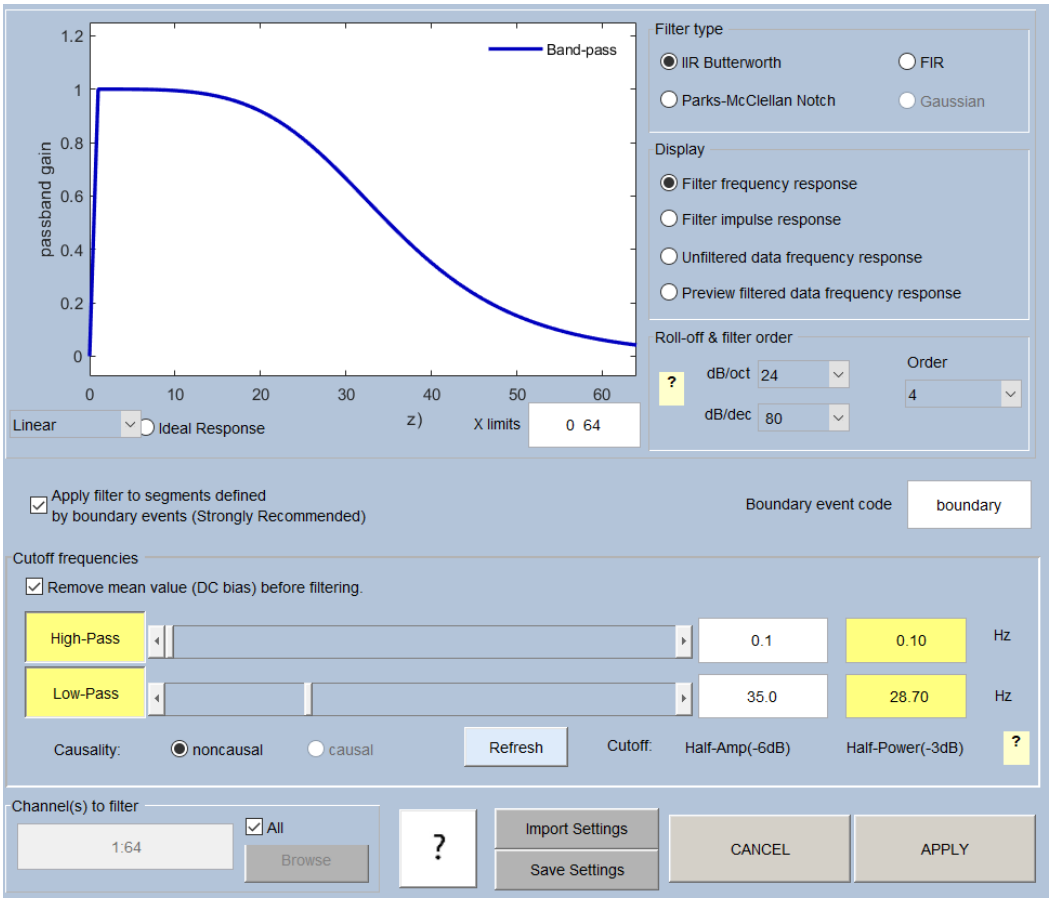

Figure 3-6 Butterworth Bandpass Filter Frequency Response

3.3.3 Independent Component Analysis (ICA)

ICA is a ML technique for distinguishing independent sources in a mixed signal. Unlike "Principal Component Analysis" (PCA), which seeks to maximize data point variance, ICA seeks to maximize independence, i.e., independent components. So, the technique of ICA separates the independent sources that are mixed linearly in different sensors. The method of ICA separates the embedded artifacts from the recorded EEG signals that are mixed linearly. The "cocktail party problem" is a common ICA example. The cocktail party problem refers to the literal scenario of creating a noisy environment in which people talking to each other cannot hear what the other person is saying. Figure no 3.7 shows the visual representation of cocktail party effect.

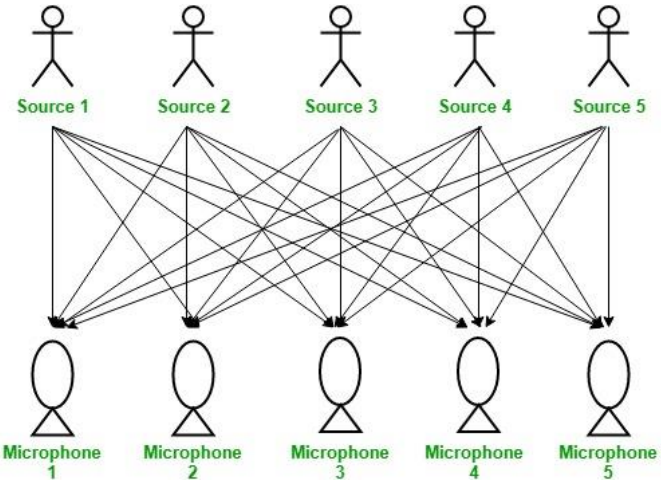

Figure 3-7 Cocktail Party Concept Visual Representation

The technique of ICA separates the audio signal from each source. In the same way the EEG signals with eye blink components, muscle artifacts line noise etc. the technique of ICA removes these artifacts from the EEG signals. In this study ICA is used by using the MATLAB ® GUI name as "EEGLAB" for the preprocessing of data for machine learning classification problem. Infomax ICA is used which removes the eye blink components from EEG data along with, muscle artifacts, heart artifacts, and line noises.

3.4 Movement Related Cortical Potentials (MRCP's)

MRCP's & sensorimotor oscillatory EEG activities that are Event related Synchronization (ERS) or Event Related Desynchronization (ERD) provides the useful information about the related

motor activities. These were first discovered by the Deecke & Kornhuber in 1964 [71]. MRCP's are negative shifting of low frequencies of range 0 to 5 Hz. in the EEG recording that occurs 1.5-2 sec before voluntary movement begins. Negative EEG activity has been associated with increased synaptic activity, so although the positive EEG activity has been linked to synaptic inactivity in the cortical area under study [71]. As a result, the MRCP's negative profile indicates an increase in cortical synaptic activity prior to movement production. The amplitude & onset time of the MRCP's premovement components are known to vary depending on the psychological & physical properties of the upcoming movement [72]. As a result, the MRCP's 2 premovement components, known as the negative slope (NS) & readiness potential (RP), & may reflect cortical processes involved in the preparation & planning for voluntary movement [73]. Researchers frequently interpret the magnitude of the negativity as an indication of the amount of energy or effort required to plan the performance of the upcoming movement [74]. Similarly, the MRCP onset time may indicate the amount of time it took to prepare & plan the movement [75]. The MRCP's includes 3 events known as motor potential (MP), readiness potential (RP) or (BP), & movement-monitoring potential (MMP), which are assumed to represent motion planning/preparation, implementation, & performance control, in that order. Figure no. 3.8 represents the MRCP plot for hand motion the BP1 represents the early BP and BP2 represents the late BP. 0 sec is the time from where the motion starts.

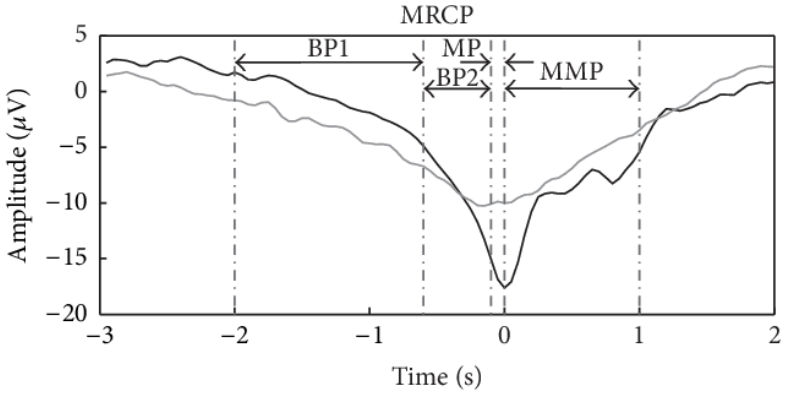

Figure 3-8 Movement Related Cortical Potential

3.5 Feature Extraction

For the classification of reach and grasp motions using machine learning techniques, hand-crafted feature set is required because ML algorithms works on the hand-crafted feature set. So, in this study the time domain hand-crafted feature set is used. The most commonly used features

from the time domain are statical features that are: mean, median, mode, standard deviation, kurtosis, skewness & similar [76]. Zero-crossing is another time domain features. It is neither a statistical nor a simple feature [77]. It represents the number of times the signal crosses the x-axis. The period-amplitude analysis is based on the examination of half-waves, or signals between two zero crossings. The wave duration, number of waves, peak amplitude, & instantaneous frequency can all be calculated using period amplitude analysis [78]. Table no 3.1 represents the time domain features that are used in this study.

Table 3:1 Time domain features

Time Domain Features	**MATLAB® Function**	**Formula**
Mean	mean(X)	$= \frac{Sum\ of\ terms}{number\ of\ terms}$
Medina	median(X)	$= \begin{cases} X\left[\frac{n+1}{2}\right] & if\ n\ is\ even \\ \frac{X\left[\frac{n}{2}\right] + X\left[\frac{n}{2}+1\right]}{2} & if\ n\ is\ odd \end{cases}$
Mode	mode(X)	$= L + h\ \frac{(f_m - f_1)}{(f_m - f_1) + (f_m - f_2)}$
Variance	var(X)	$= \frac{\sum(x_i - \bar{x})^2}{n-1}$
Standard Deviation	std(X)	$= \sqrt{\frac{\sum(x_i - \mu)^2}{N}}$
Minimum	min(X)	____
Maximum	max(X)	____
Kurtosis	kurtosis(X)	$= \frac{\mu_4}{\sigma^4}$
Skewness	skewness(X)	$= \frac{\sum_i^N (X_i - \bar{\bar{X}})^3}{(N-1) * \sigma^3}$
Mean Absolution Deviation	mad(X)	$= \frac{1}{n}\sum_{n=1}^{n} \lvert x_i - m(X) \rvert$

3.6 Classification

The feature set for machine learning models is then used to decode reach and grasp motions. The data was then evenly divided into two classes: reach movement & grasping movement. The following section describes the various decoders that were used.

3.6.1 Machine Learning Methods

3.6.1.1 Support Vector Machine (SVM)

SVM is applied to create the best hyperplane with the greatest margin for dividing data between two clusters. A single hyperplane is sufficient to divide two-dimensional data into two groups, such as +1 or -1. According to Figure no. 3.9, two hyperplanes are required to distinguish the data points for three-dimensional data. SVM creates a hyperplane to separate the sample data into target categories.

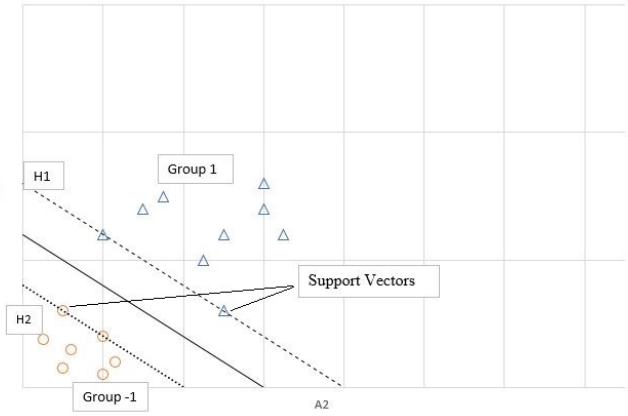

Figure 3-9 SVM Linearly Separable Method

There are several possible linear hyperplanes for 2D data, & the optimal hyperplane with the greatest margin width must be found. H1 & H2 are parallel to the optimal hyperplane & represent the distance between the hyperplane & the data points. Margin is defined as the distance between the dotted lines (AC). Support Vectors (SVs) are some of the sample data points that lie on the hyperplanes H1 & H2. Refer to figure 3.7 for more information. These SVs are required to calculate the width of margin. [79] asserts that linearly separable classification divides high-dimensional data into two groups, $(y_1 = +1, -1)$ with no overlapping or misclassification. Equations 3.2 & 3.3 are used to represent the H1 hyperplane & H2 Hyperplane.

$$w_1 x_1 + w_2 x_2 - b = 1 \quad (3.2)$$

$$w_1 x_1 + w_2 x_2 - b = -1 \quad (3.3)$$

In the above equations w_1 & w_2 represents the positions of the hyperplanes of H1 & H2 respectively and x_1 & x_2 represents the data points whose values are -1, 0, +1 that represents how

far the hyperplane line lies away from the point of origin or original point of line. The minimum and maximum margin widths are $\frac{1}{w}$ & $\frac{2}{w}$ respectively.

$$y_i(w_1x_{i1} + w_2x_2 - b) \geq 1 \quad for\ i = 1,2,3,\dots m \tag{3.4}$$

The Lagrangian multiplier can be defined by equation as:

$$L(w,b,a) = \left[\frac{1}{2}w^2 - \sum_{i=1}^{n} a_i[y_i w'^{x_i} + b] - 1]\right] \tag{3.5}$$

This means that

$$w = \sum_{i=1}^{n} a_i\, y_i x_i \tag{3.6}$$

Hence the equation 3.7 defines the classifiers optimal Decision Function that is:

$$f(y) = sign(\sum_{i=1}^{sv} a_i y_i (x_i x_s v) + b) \tag{3.7}$$

3.6.1.2 Linear Discriminant Analysis (LDA)

For classification in LDA, a classifier employs the Bayes' theorem. The discriminant analysis calculates the Gaussian distribution parameters for each class, & the trained classifier selects the class with the least misclassification cost. The product of the prior probability & multivariate normal density yields the posterior probability that a point x belongs to class C. At a point x, the density function of the multivariate normal with mean & covariance is given by:

$$P(x|C) = \frac{1}{(2\pi|\sum c|)^2} exp\left(-\frac{1}{2}(x-\mu_c)^T \sum_c^{-1}(x-\mu_c)\right) \tag{3.8}$$

If P(C) symbolizes the prior probability of the class C, then the observation's x posterior probability of class C is given by:

$$P(C|x) = \frac{P(x|C)P(C)}{P(x)} \tag{3.9}$$

R. A. Fisher invented the LDA model. The linear method (LDA) uses the same covariance matrix for every class, with only the means differing. Both the covariances & means of each class vary in quadratic discriminant analysis (QDA).

3.6.1.3 K-Nearest Neighbors (k-NN)

k-NN is one of the most basic classification algorithms. The classification of a feature vector is determined by the majority vote of its neighbors. The object class is assigned to the most common one discovered among k nearest neighbors. For example, class "square" is shown in the Figure no. 3.10.

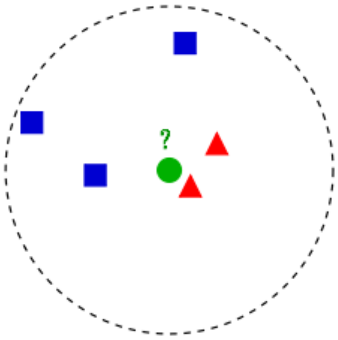

Figure 3-10 k-NN classier for classification of object with k=5

3.6.2 Deep Leaning Methods

The “Keras” library is used to implement the deep learning portion of this research, with the “TensorFlow” library serving as a backend. On the reach and grasp motion dataset, a 2D deep CNN model is developed and tested, as well as the results with two other DL models. While they have a similar overall structure and design, they differ in depth, width, and the number of parameters. This section discusses the decisions made in the design of the proposed CNN model.

3.6.2.1 Architecture of CNN model

A deep learning CNN model is proposed in this study which classifies the Reach and Grasp motion from neural corelates. The design of the proposed model is shown in Figure no. 3.11. The model consists of 2D convolutional layers along with average pooling layers, and separable convolutional layers, followed by the fully connected layer. First layer C1 is input layer, the input shape used for the model is time series data in the form of Channels x Time Points (C x T). Second layer or C2 is of 2D convolutional layer along with bath normalization layer. It consists of 8 filters of size (1,64) which moves along the time axis for extracting the feature values. The feature map of C2 layer is used as a input for third layer C3 that is separable convolutional layer with 32 filters of size (1,64), these are doing depth and point wise convolution this layer extracts the time features depth and point wise, next to separable 2D convolutional layer is Bath normalization layer with activation function “ELU”. Forth layer C4 is average pooling layer with filter size (1,8). This layer reduces the complexity of the feature map then a dropout layer is applied with 0.2 dropout value. Fifth layer C5 is again separable convolutional layer with 16 filter of size (1,16) and then again apply bath normalization layer with activation function “ELU”. Then again average pooling layer is applied for reducing the complexity of feature map.

Sixth layer C6 is flatten layer which combines the output of C5 into vector & the seventh layer C7 is a fully connected layer. Lastly the “Sigmoid” layer is added in the model that predicts the probability distribution of output classes i.e., Reach & Grasp actions. Detail about the activation function, optimizer, and layers used are given below. The detail of the architecture is given in appendix A.

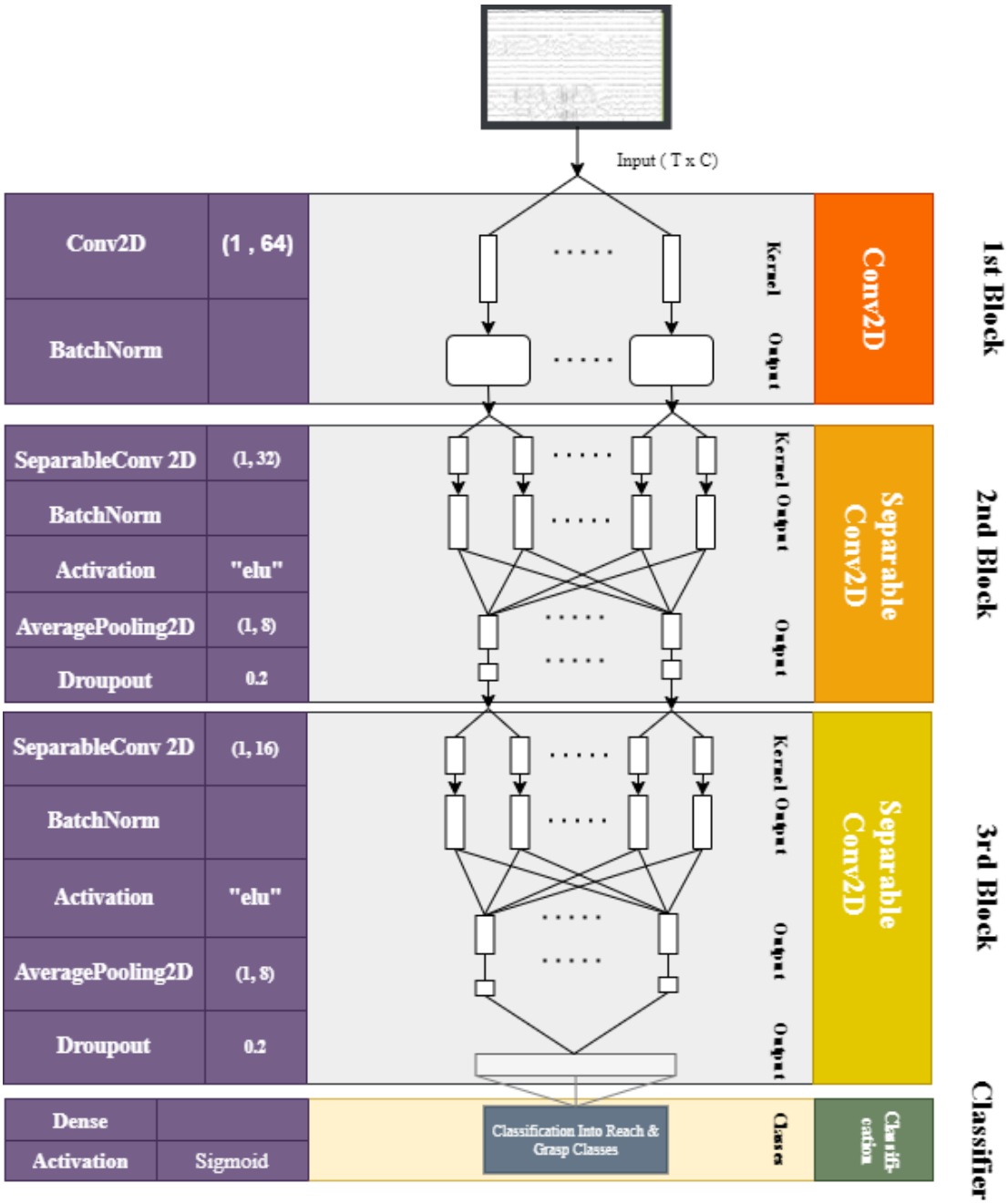

Figure 3-11 Architecture of Proposed Model

I. Activation Function

Recently in most of the EEG classification NN models, the most used activation function in Exponential Linear Unit (ELU). ELUs, unlike "ReLUs", have negative values, allowing them to push mean unit activations close to zero. Just like the technique of "batch normalization" but in in case of "ELU" less computational power is used because of less computational complexity [80]. Because of the reduced bias shift effect, shifting of mean toward zero accelerate learning by bringing the normal gradient closer to the unit natural gradient. Mathematically, the equation no. 3.10 & 3.11 defines the "ELU" function:

$$y = ELU(x) = \exp(x) - 1 \; ; if \; x < 0 \tag{3.10}$$

$$y = ELU(x) = x \; ; if \; x \geq 0 \tag{3.11}$$

Graphically, Figure no. 3.12 represents the activation function "ELU":

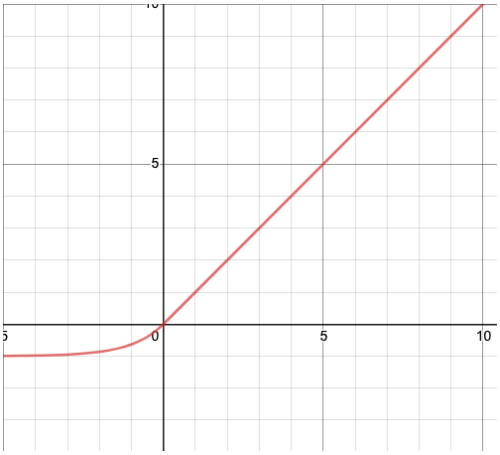

Figure 3-12 ELU activation function curve [80]

II. Dropout Regularization:

In the deep learning model's overfitting is a very common problem specially in CNN models. One of the method to reduce the effect of over fitting of model was introduced by the Srivastava et al. [] that is through Dropout Regularization (DR). DR is the process of randomly removing units and their connections from the network during each training step. When a layer has 50% dropout, each unit in that layer has a 50% chance of being deactivated at each training step.

The concept behind DR is that by training networks of different configurations & using their average output for prediction, one should be able to neutralize overfitting, but for complex

architectures, this is impossible. Dropout enables us to approximate the average of an exponentially large number of networks. With a 50% dropout rate, the network is trained with a slightly different architecture at each step, with the net result being an average of all these different architectures.

III. Loss Function:

The Loss Function used in prosed model is "Binary Cross-entropy". This is commonly used for the binary class classification problems. There are multiple problems with only two answers so for that this is use d. In this thesis binary class classification is performed for classification of "Reach" and "Grasp" motions. It is defined as the "Negative average of log of corrected predicted probabilities". This loss is equivalent to the average of the categorical cross entropy loss on many 2 category tasks. Mathematically binary Cross-Entropy is defined by equation 3.12:

$$Loss = -\frac{1}{Output\ size}\sum_{i=1}^{output\ size} y_{i.} log\hat{y_i} + (1 + y_i).\log(1 - \hat{y}_i) \qquad (3.12)$$

Here:

$\hat{y}_i$ is mode's output $i - th$ value

y_i corresponding targeted value

IV. Optimizer:

The optimizer used in proposed model in "Adam" that was introduced by Jimmy Ba & Diederik Kingma from Toronto University & Open AI respectively in 2014 [81]. The name of optimizer "Adam" is developed from "Adaptive Moment Estimation". Adam optimizer is different from the classical SGD (Stochastic Gradient Descent" optimizer. For all weight updates, SGD maintains a single learning rate (lr) called as alpha, which does not change during training process. Each network weight or parameter has its own lr that is adjusted as learning progresses. Adam is made by combing the advantages of Adaptive Gradient Algorithm (AdaGard) that improves the performance by maintaining the pre-parameter lr & the Root mean square propagation (RMSprop) that also pre-parameters lr on the average of recent magnitudes of gradients for the weight. In this way the method performs best for both nonstationary (like EEG) & online problems. These both are the extension of SGD. So, Adam realizes the advantages of both RMSProp & AdaGard.

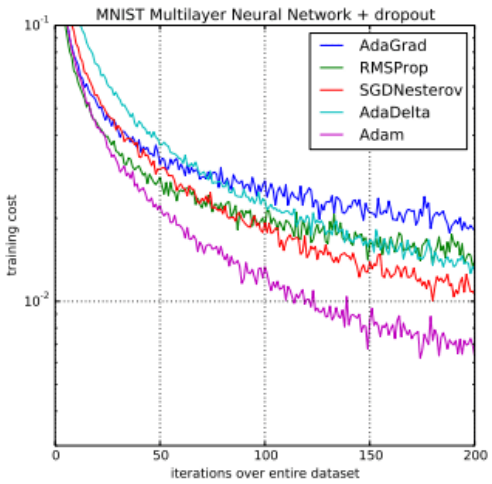

Figure 3-13 Comparison of MLP training using other Optimizers with Adam [81]

V. Training & Validation

Accuracy, or how many of the objects in the data set were correctly classified, is the most common measure of success in any machine learning & Deep Learning problem. A ML or DL algorithm may achieve very high accuracy on the training set while failing to generalize to new data, necessitating some method of validating the algorithm. Validation is required to accurately determine the performance of any ML or DL method. This is typically accomplished by dividing the data set into 2 parts: a training set, on which the data is trained, & a testing set, on which the model is tested after training. The dataset can be divided in an infinite number of ways. It must be large enough to accurately represent the data while not being so large that we have insufficient training data. An average split is 80% for training data & 20% for testing data []. In this thesis for ML models are trained and tested on small data because most of the trails got rejected on the basis of peak amplitude threshold value, abnormal kurtosis & abnormal joint probability values. So, there is another advance approach of validation is applied on ML models that is "cross validation approach". In this technique the model of ML is trained repeatedly on multiple subsets of the training dataset. The most used technique in cross validation is the one that is used in the research called as "k-fold cross validation approach". Figure no. 3.13 shows the diagram of 5-fold cross validation approach

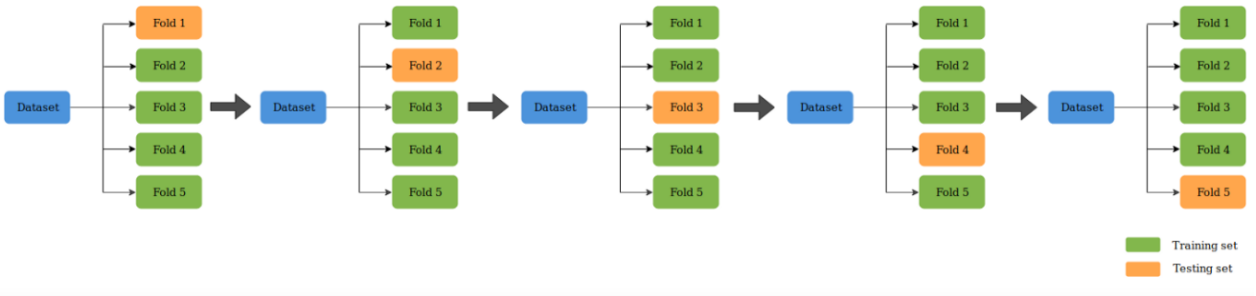

Figure 3-14 5-fold cross validation approach. Green represents the training data sets and orange represents the test subset.

For the DL models the simple validation approach is used because in DL model's raw data is used as an input so there is no loss of data while trail rejection. For DL & ML models 70:30 split ratio used for training and testing of models.

CHAPTER 4: RESULTS AND DISCUSSION

4.1 Pre-Processing

For the preprocessing of EEG data MATLAB® toolbox EEGLAB is used. Firstly, the data is loaded and then channels list and events list are uploaded after that the spatial filtering technique of Common Average Referencing (CAR) filter is applied on the data of Gel based recordings for all the 15 subjects one by one. The CAR filter is enough to extract cortical potentials of sensorimotor cortical activities modulated by the user's intention. Then the 4^{th} order Butter worth filter with frequency range 0.01 Hz to 35 Hz. are applied on all the available EEG and EOG channels Figure no. 3.4 and Figure no. 3.5 shows the raw and filtered EEG data.

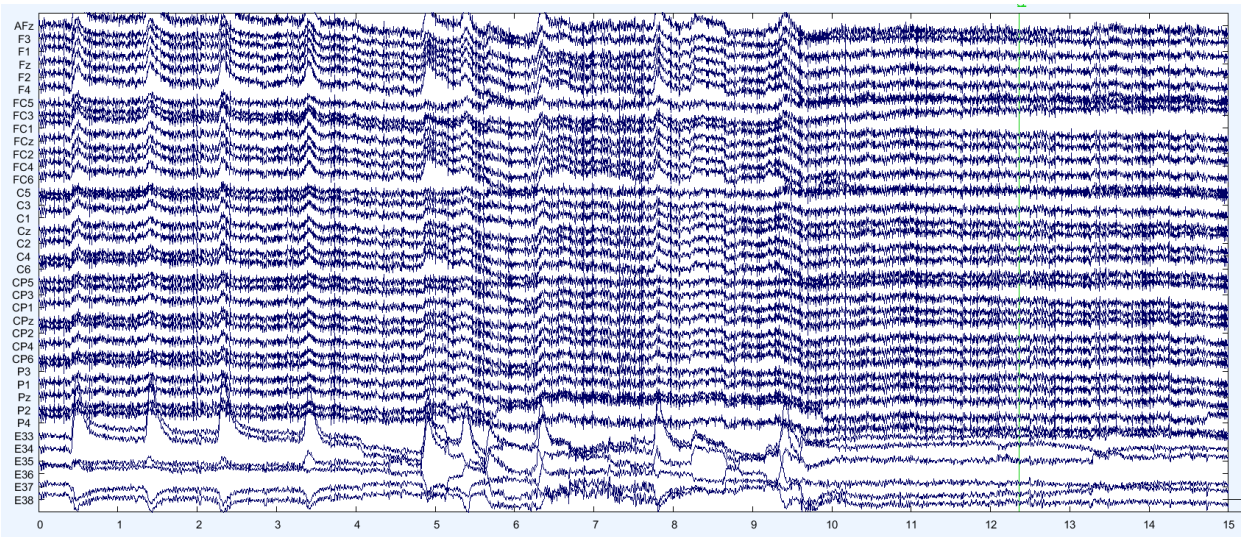

Figure 4-1 Gel based EEG datasets recordings from 64 channels. (Raw Signal)

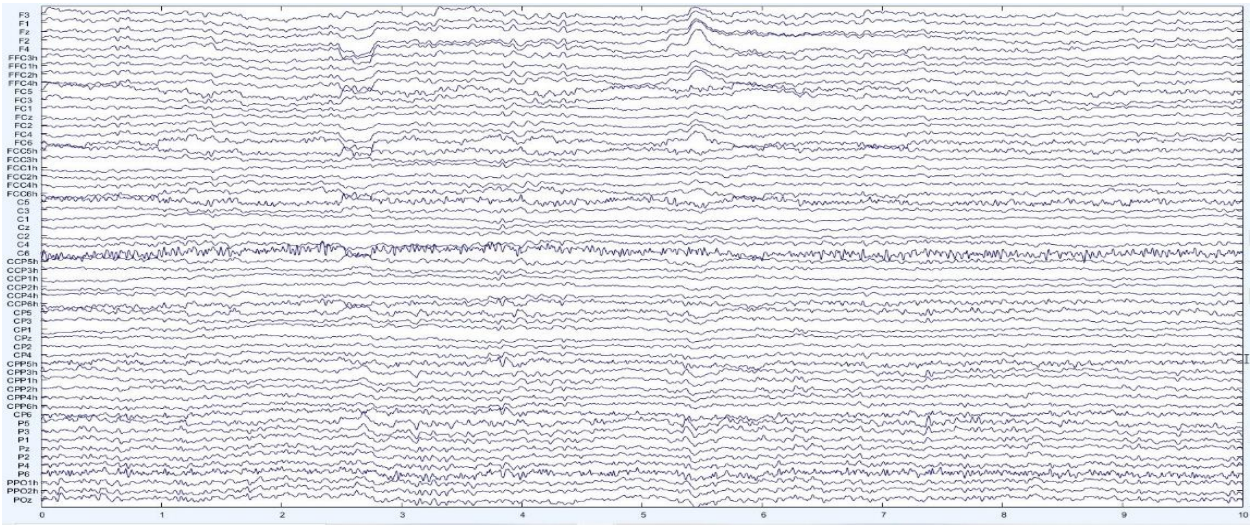

Figure 4-2 Gel based EEG datasets recordings from 58 channels. (Filtered Signal)

Then for removing the line noise from the data the line uses the “Cleanline” plugin of EEGLAB Figure no. 3.6 shows the Power Spectral Density (PSD) of filtered signal without applying Cleanline filter. It is clearly visible that there are artifacts of line noise at 50 Hz. frequency.

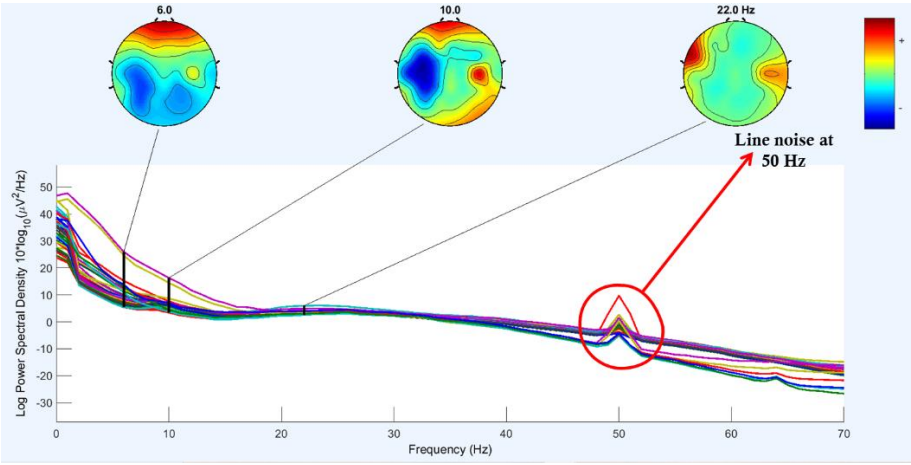

Figure 4-3 Power Spectral Density (PSD) of filtered EEG signal (with line noise)

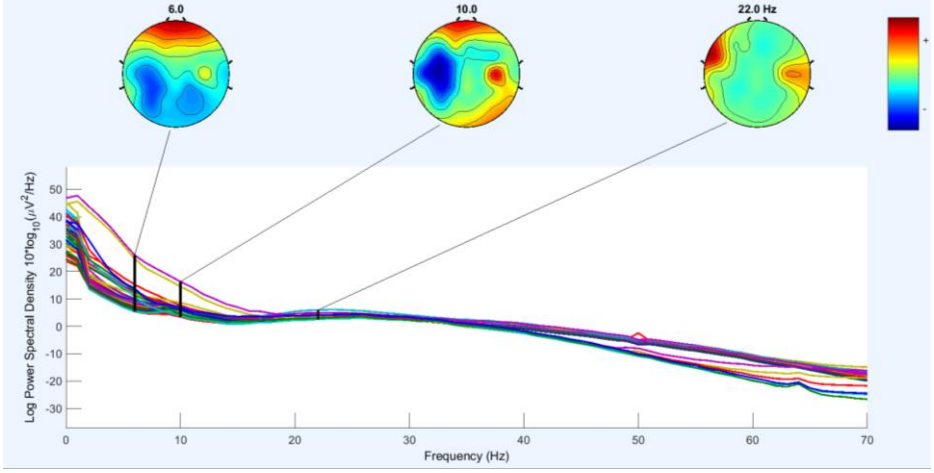

Figure 4-4 Power Spectral Density (PSD) of filtered EEG signal (After applying Cleanline plugin)

After removing the line noise artifacts from EEG data, the eye blink components along with the muscle artifacts components, channel noise are removed from data by using the ICA algorithm. The ICA is applied by using the EEGLAB from there the infomax ICA technique is used then the components are labels by using the “IClabel” pretrained model that classifies the components into different classes. Figure no. 4.5 shows the labeled ICA components which shows multiple classes like eye, channel noise, muscle brain etc. from all these classes eye, muscle, line noise will be removed. The figure no. 4.6 (a) shows the EEG signal plot before (blue line) and after (red line) the ICA components removed. The blue lines clearly show the artifacts in brain signals

and these are removed after removing the ICA components of eye, line noise etc. as shown by red line signals.

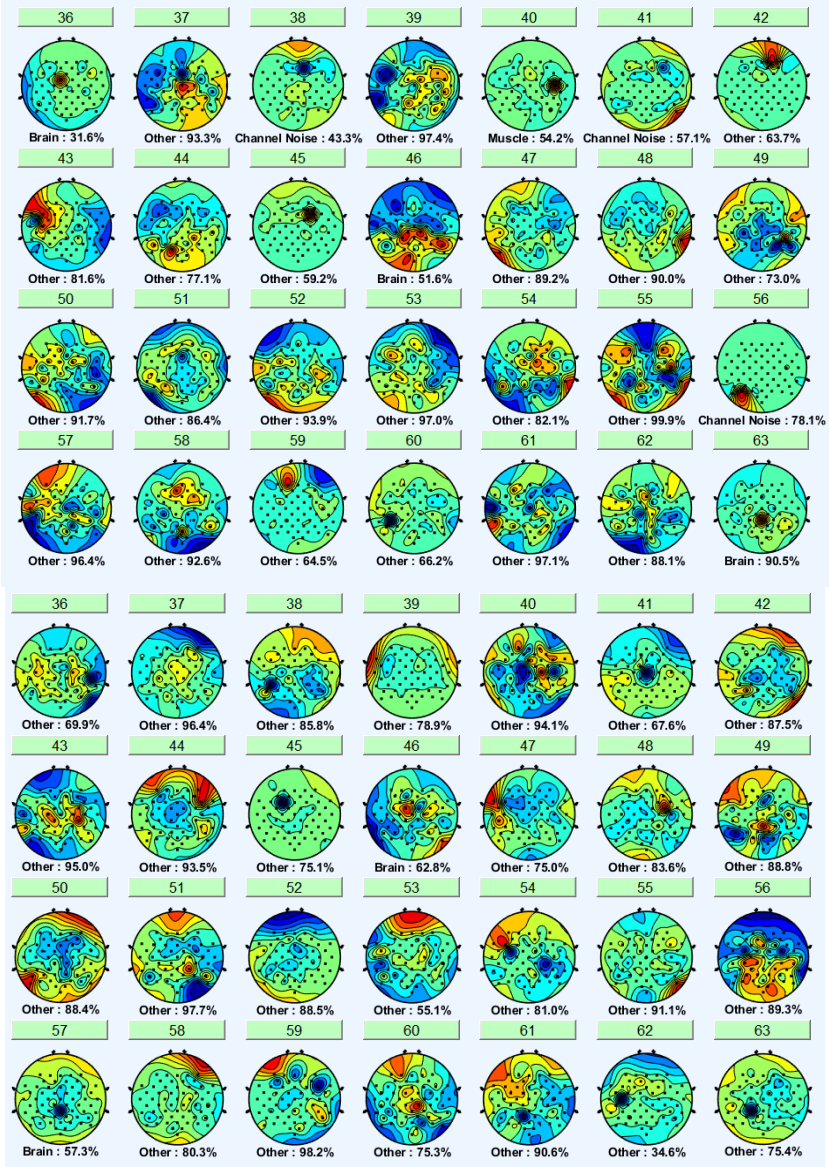

Figure 4-5 Labeled ICA components of EEG data

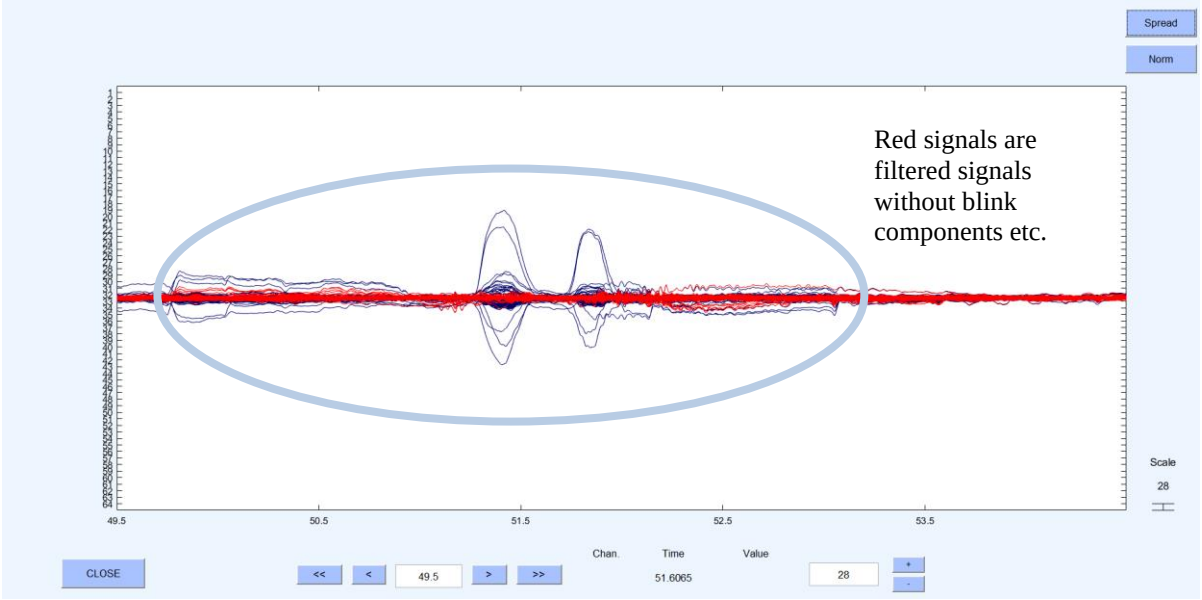

Figure 4-6 EEG signals before (blue) and after (red) removing ICA components. Region in circle shows the artifacts part.

After removing the ICA components, the data is then down sampled to 26 Hz. from 256 Hz. for saving the computational power. After that the EOG channels are removed from the data by interpolating the channels.

Figure 4-7 Interpolating of Channels

After removing the EOG channels the trails of “Reach” and “Grasp” motions are then extracted from the continuous EEG data. The epoch trails are then rejected based on peak amplitude threshold i.e., 125uV, abnormal joint probability & finally based on abnormal kurtosis

by threshold of 5 times the standard deviation, the rejected trails, & their details for Subject 4 in shown in Figure no. 4.8 & 4.9.

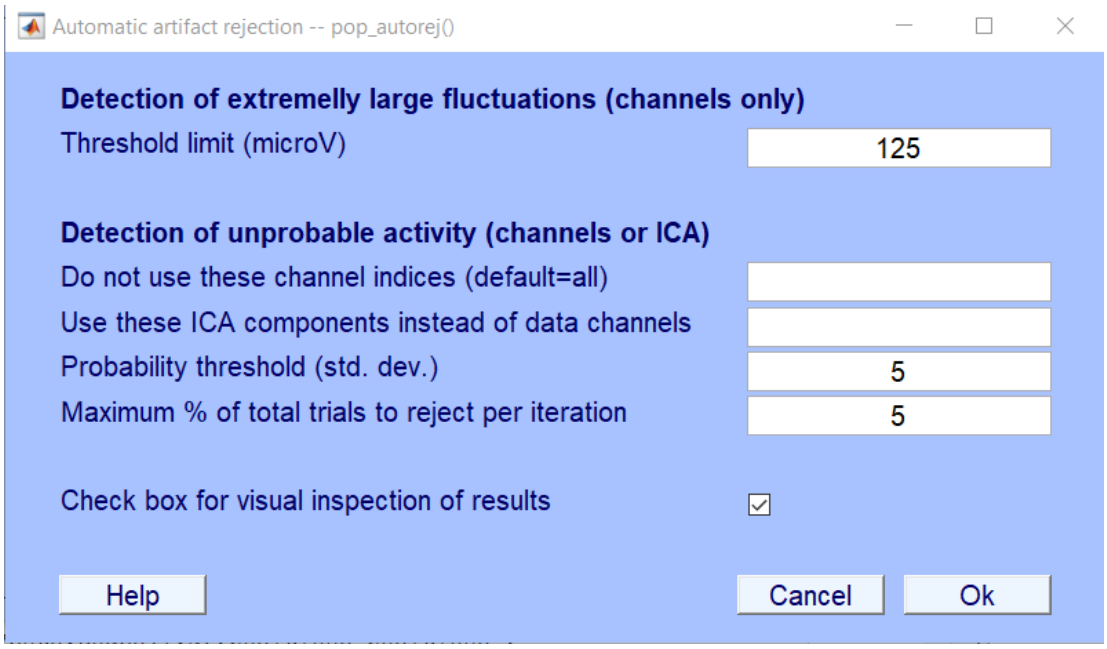

Figure 4-8 Epoch rejection with 125 uV threshold amplitude, abnormal joint probability and abnormal kurtosis

```
10/267 trials marked for rejection
10 trials marked for rejection
```

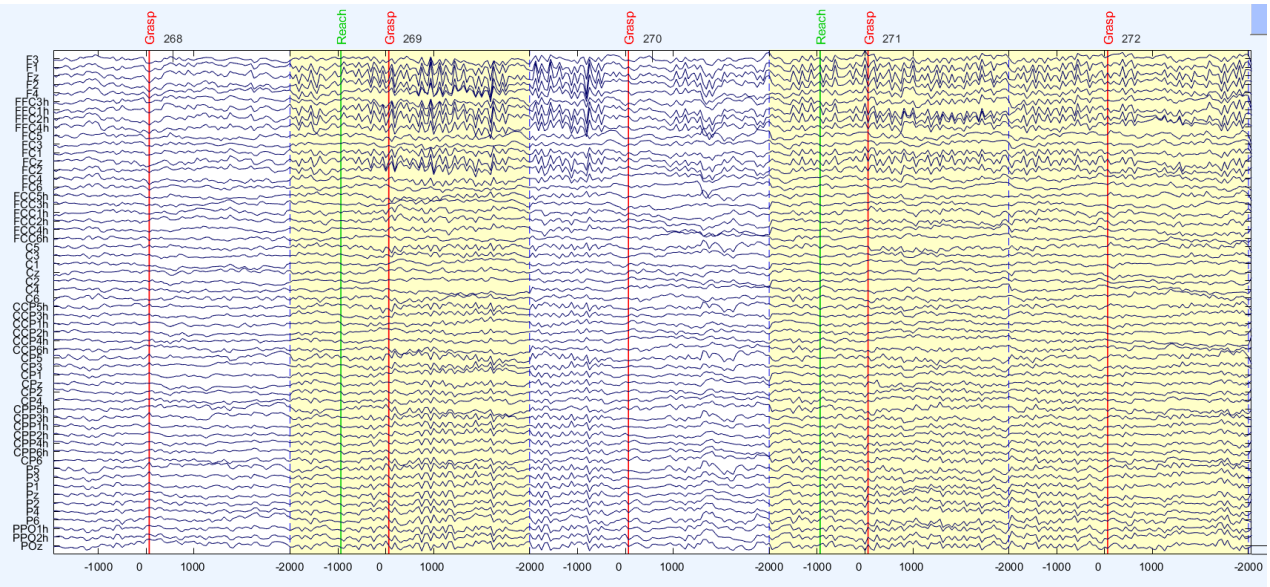

Figure 4-9 Rejected trails of Grasp action for Subject 4 based on peak amplitude threshold value, abnormal kurtosis and joint probability Highlighted trails show the rejected trails

MRCP's are used to differentiate movements of different hand motions or limbs by measuring changes in Potential distribution from brain signals. To calculate & decode MRCPs for reach and grasp actions, EEG signals from EEG recordings are resampled to 16 Hz to save computational power, & then the CAR filter is applied again. The EEG signals are then subjected to a Moving averaging filter of 2nd order. The MRCP values are calculated from each channel, with the exception of the mean confidence interval & the mean over all trails of each subject for each movement condition type. The mean value over the subject specific averages is used to calculate the grand average for each type of available EEG dataset. All Reach and Grasp trails are epoched according to the window of interest (WOI) , i.e. [-2 3] sec. The non-parametric t-percentile bootstrap statistics are used to calculate the 95% confidence interval for each movement condition. The MRCP's are plotted for motor cortex channels that are FCz, C1, Cz and C2 shown in Figure no. 4.10.

4.2 Feature Extraction

For the ML models the feature set is extracted from the segmented trails of reach and grasp. As a feature set 11 amplitude values and band power of signal are taken from all the available EEG channels i.e., 58 channels. The total features extracted from recordings are 638 features (11 x 58 channels).

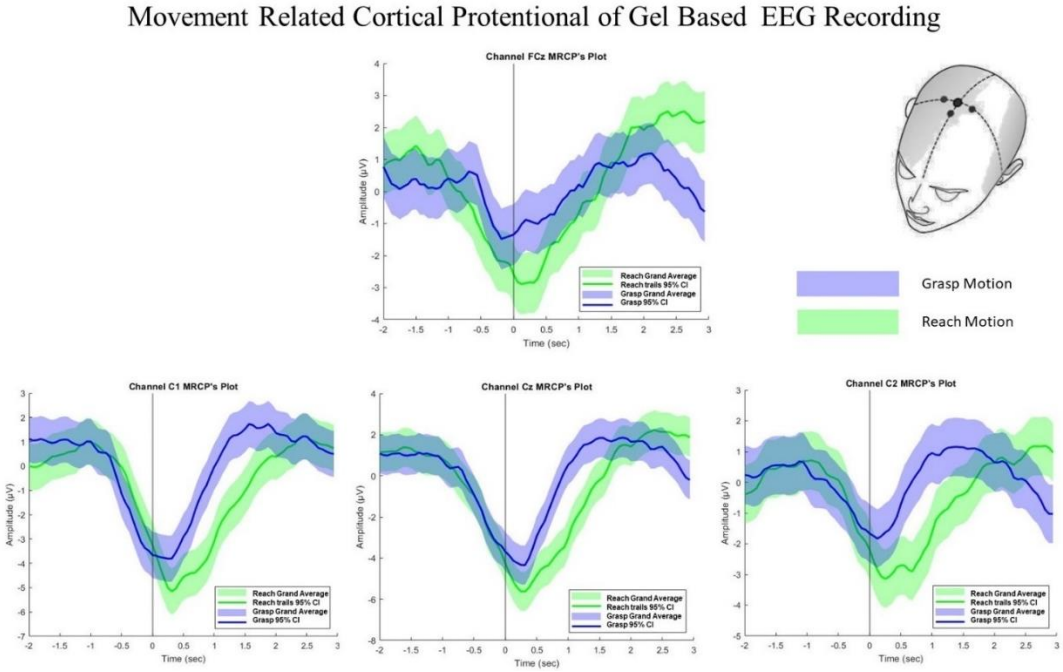

Figure 4-10 Movement Related Cortical Potentials (MRCP's) for Reach and Grasp Actions of Channel FCz, C1, Cz, and C2. Green line shows the MRCP of Reach action and blue lines shows the MRCP of Grasp actions.

4.3 Machine Learning Classifiers

After extracting the features, the machine learning classifiers are applied to them for each subject one by one. In this thesis LDA, SVM and K-NN models are applied. All the features are extracted from the preprocessed data subject of each subject with 70:30 split ratios. For every subject 5-fold cross validation approach is used in which the training data is divided into 5 groups and in each iteration one group is sued for testing and remaining 4 are used for training of model. The accuracies of all the subjects are tested on the 3 models LDA, SVM and k-NN. Table no 4.1 shows the test and training accuracies of all the 15 subjects on LDA, SVM and k-NN classifiers. It is visible from the results that the k-NN shows the overall best classification accuracy as compared to LDA and SVM classifiers. Figure no. 4.11 shows the comparison graph of 3 different ML classifiers. On the hand-crafted feature set k-NN classifiers shows the best classification results on unseen data.

Table 4:1 Classification accuracies of 15 Subjects using LDA, SVM and K-NN Machine learning Models

Classifiers / Subjects	**Linear Discriminant Analysis classification (%)**		**Support Vector Machine classification (%)**		**K-Nearest Neighbor Classification (%)**	
	Training	**Test**	**Training**	**Test**	**Training**	**Test**
G01	65.2	63.7	67.8	66	79.8	77.6
G02	63.4	60.8	68	67.8	77.4	76.0
G03	64.2	60.8	66.4	65.2	84.4	81.4
G04	71.2	69.1	69.6	68.8	80.2	79.1
G05	63.4	60.3	67.4	68.3	81.3	79.6
G06	65.3	64.9	70.2	69.1	81.4	80.7
G07	60.6	56.2	67.4	67.2	76.9	75.8
G08	55.2	53.8	62.9	61.0	78.5	83.8
G09	64.5	62.8	70.6	68.4	74.4	74.6
G10	60.2	60.1	65.4	62.9	72.6	76.3
G11	60.2	61.6	68.5	66.5	77.4	82.8
G12	58	55.7	66.6	68.0	76.3	80.9
G13	66.2	60.7	73.5	72.1	81.4	82.2
G14	62.7	58.6	67.7	67.1	81.7	84.2
G15	66.2	62.4	65.3	62.6	79.8	82.2
Average	**63.1 ± 3.86**	**60.77 ± 3.80**	**67.82 ± 2.53**	**66.73 ± 2.86**	**78.9 ± 3.11**	**79.81 ± 3.11**

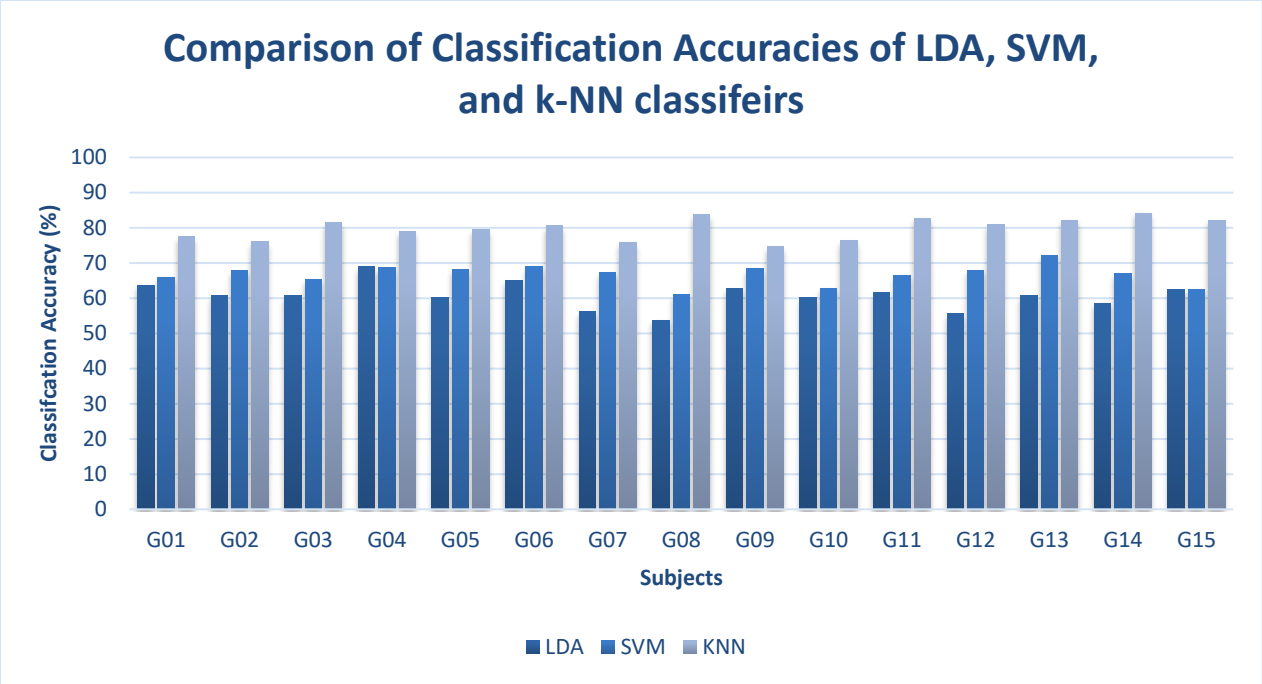

Figure 4-11 Comparison of test accuracies of LDA, SVM and K-NN classifiers

4.4 DL CNN based Classification

For the deep learning model raw EEG data is used with simple pre-processing steps that includes the 4th order Butterworth bandpass filter with cutoff frequencies 0.1 to 35 Hz. After that the data is segmented and that segmented data is used as an input from the Deep learning CNN model. The data is split into training and test sets with 70:30 ration. The] models of DL in previously used in literature also tested on this dataset for comparing the accuracy of proposed model. The models of CNN proposed in literature related to edge device perspective are also used are DeepConvNet [82], and EffNet [83]. Figure no. 4.12 shows the comparison of size of proposed CNN model with models proposed in literature for the edge device perspective. Size wise the proposed model is much batter then the other models that usually used for Motor actions classification from EEG signals.

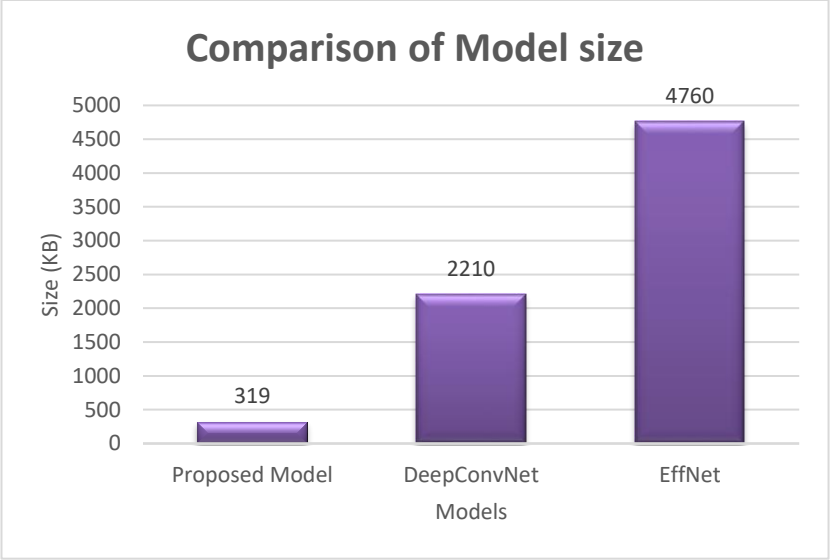

Figure 4-12 Comparison of Model sizes (KB)

Table 4:2 Number of parameters in different DL models

Model Name	***No. of Parameters***
Proposed Model	20833
DeepConvNet	184726
EffNet	399073

The EffNet is specially proposed for the edge device perspective but still its size is much bigger than our model. The number of parameters of each model is given in table no 4.2. As it is clear from table 4.2 that the number of parameters of proposed model is far lesser as compared to EffNet and DeepConvNet, here the classification accuracy of proposed model shows better results than the other 3 models of DL. Figure no. 4.13 shows the classification accuracy of 15 subjects on Proposed model, DeepConvNet, and EffNet models. From the results of figure 4.13 & 4.14 the proposed technique shows the batter classification accuracies as compared to DeepConvNet which shows greater average classification accuracy but because of greater number of parameters and large model size this model will use more computational power.

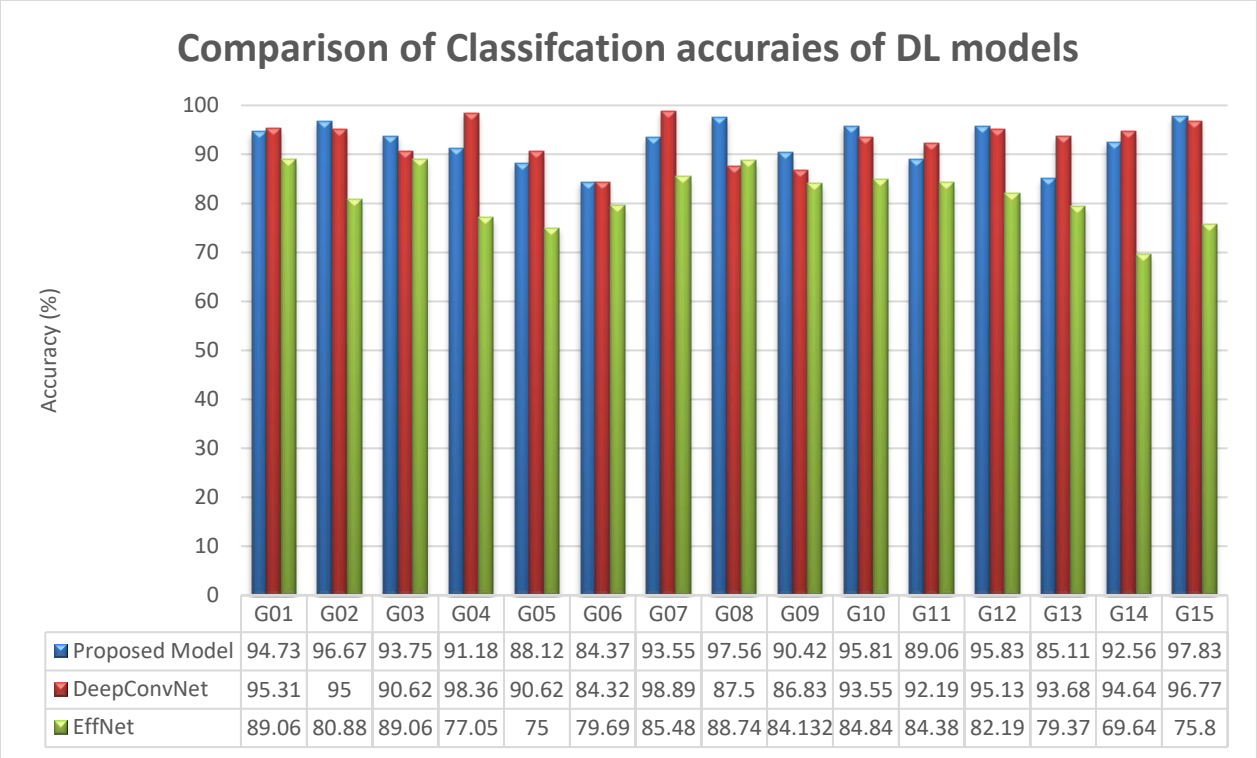

	G01	G02	G03	G04	G05	G06	G07	G08	G09	G10	G11	G12	G13	G14	G15
Proposed Model	94.73	96.67	93.75	91.18	88.12	84.37	93.55	97.56	90.42	95.81	89.06	95.83	85.11	92.56	97.83
DeepConvNet	95.31	95	90.62	98.36	90.62	84.32	98.89	87.5	86.83	93.55	92.19	95.13	93.68	94.64	96.77
EffNet	89.06	80.88	89.06	77.05	75	79.69	85.48	88.74	84.132	84.84	84.38	82.19	79.37	69.64	75.8

Figure 4-13 Subject wise classification accuracies of DL models

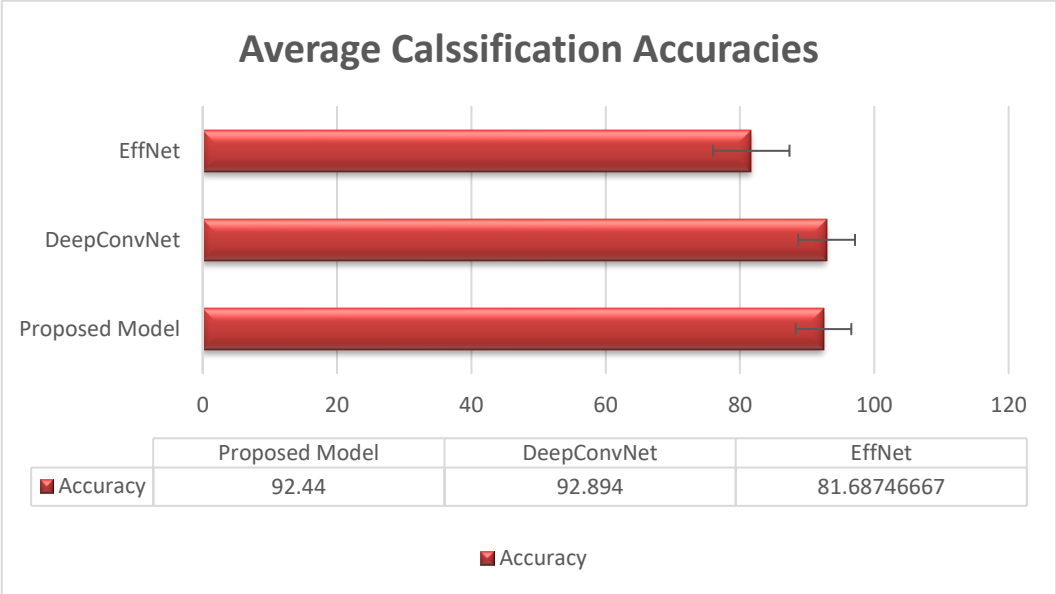

	Proposed Model	DeepConvNet	EffNet
Accuracy	92.44	92.894	81.68746667

Figure 4-14 Average classification accuracy of different DL models

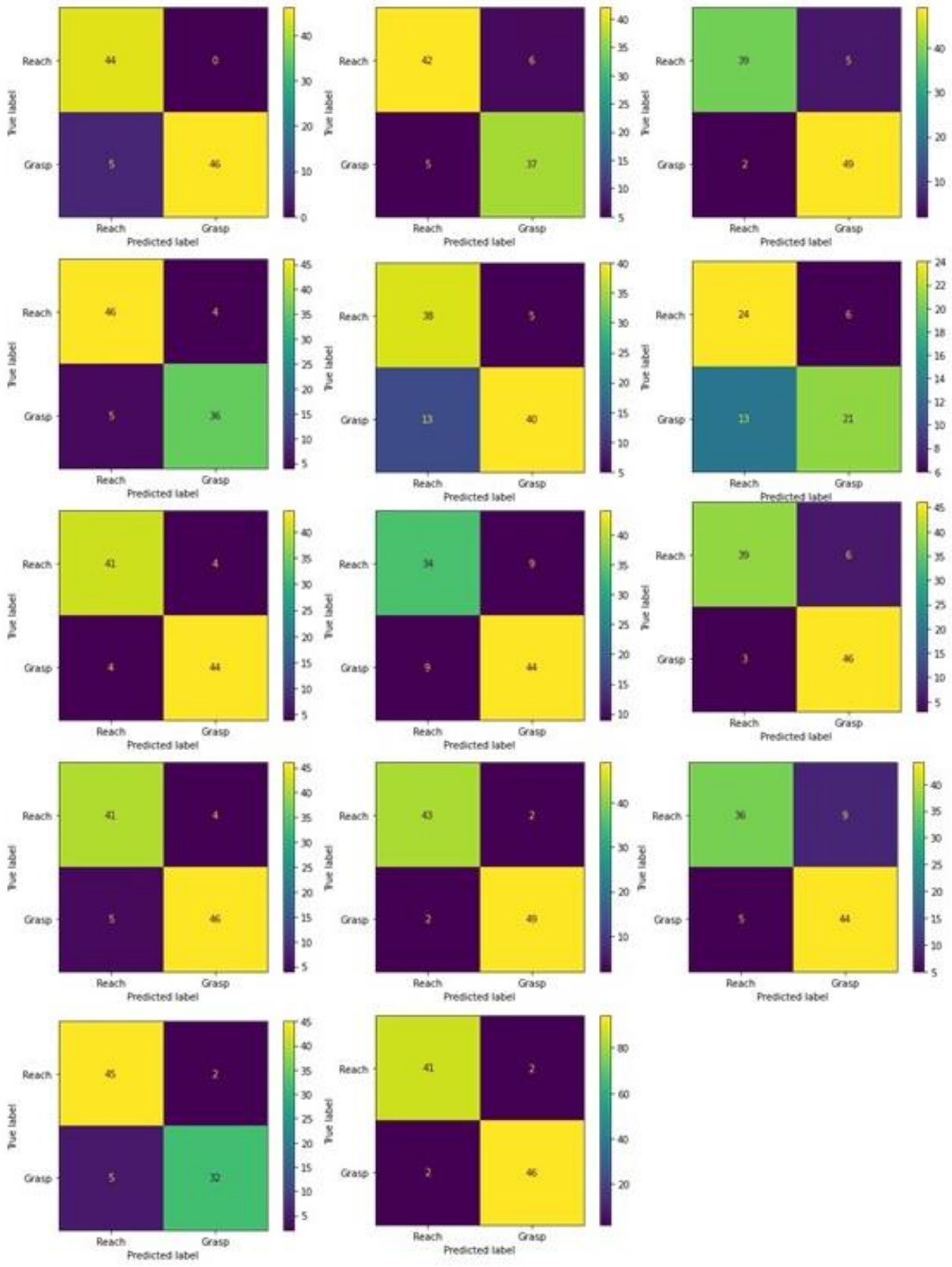

Figure 4-15 Confusion Matrix of reach and Grasp action of Proposed Model of 15 Subjects

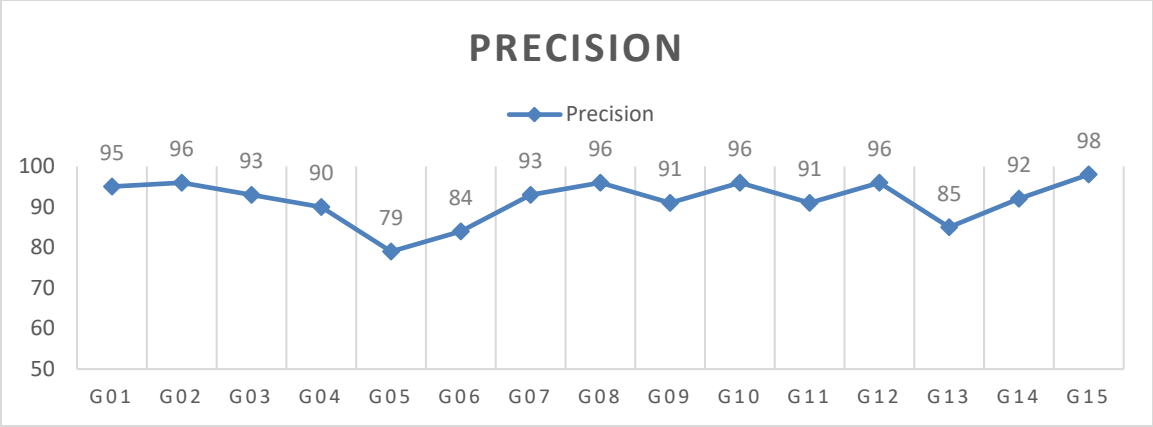

Figure 4-16 Precision of 15 Subjects on Proposed Model

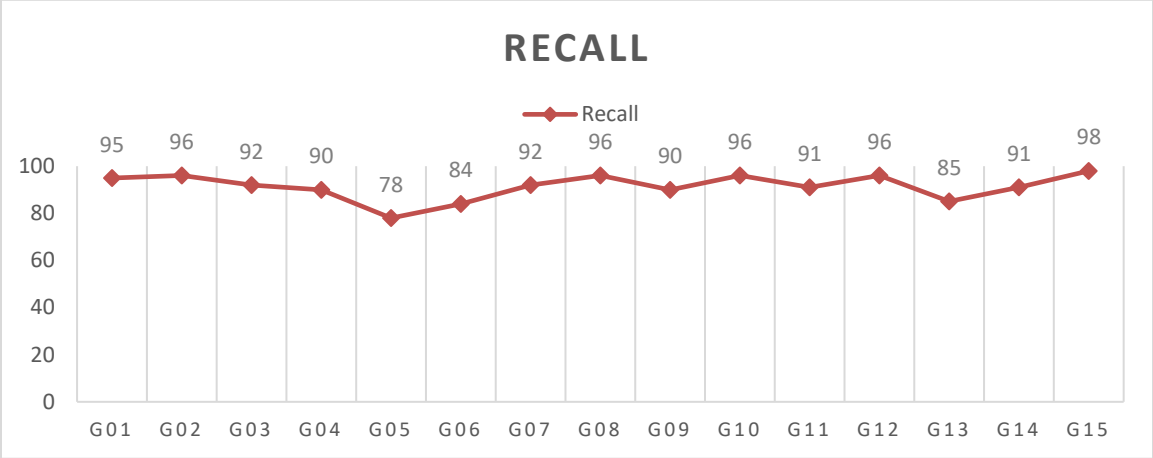

Figure 4-17 Recall of 15 subjects on proposed model

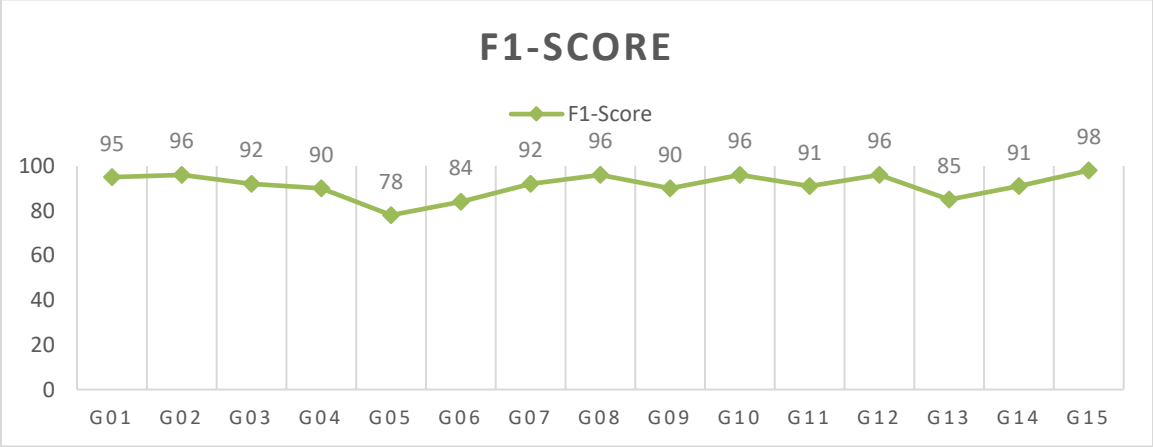

Figure 4-18 F1-score of 15subjects on proposed model

So overall, the proposed DL model shows the batter results with raw data as compared to other machine learning and deep learning models.

CHAPTER 5: CONCLUSION

This thesis compares Machine learning models proposed a deep learning model. The ML models use the hand-crafted features as an input for the classifier in this thesis LDA, SVM, & K-NN ML models are used for decoding the EEG signals for the detection & classification of different motion of same hand using the dataset that is recorded by using the Gel-based recording system. But the focus of the thesis is the classification of raw signals using deep convolutional neural network which provides higher classification accuracy and consume less computational power so that the model can help in the development of BCI systems for the rehabilitation purposes for stroke or spinal cord injury patients. The methods of ML and DL applied subject wise. For the ML data the EEG signals are filtered using and then the ICA is also applied for removing the eye blink, line noise or muscle movements components from the recorded data and after applying these techniques and extracting time domain features of Reach and Grasp motions from the EEG signals the LDA, SVM and K-NN classifiers shows the average accuracies of 60.77%, 66.73% and 79.81% respectively on the unseen dataset.

In case of Deep Learning model that is proposed the data set is used in the raw form and very minor preprocessing steps are applied that include butter worth filter and normalization step. The raw signal is given as an input to the deep learning model and the model achieves the average classification accuracy of 92.46 % on the unseen dataset. For the compression purposes the DL models that are proposed in literature are also tested on this dataset, the models used are EffNet that is specially designed for the edge device perspective. EffNet and DeepConvNet shows the classification accuracies of 81.68% & 92.89% on unseen dataset. The DeepConvNet shows approximately the same results as that of proposed CNN model, but the number of parameters and size of model is bigger as compared to proposed technique. So, developed CNN model shows the best results and can be used in the implemented on the edge devices and use for the development of BCI system

REFERENCES

[1] T. Bonaci, J. Herron, C. Matlack, and H. J. Chizeck, "Securing the Exocortex: A Twenty-First Century Cybernetics Challenge," *IEEE Technology and Society Magazine*, vol. 34, no. 3, pp. 44–51, Sep. 2015, doi: 10.1109/MTS.2015.2461152.

[2] E. Karls, "Gedruckt mit Genehmigung der Mathematisch-Naturwissenschaftlichen Fakultät der."

[3] C. Park, D. Looney, N. Ur Rehman, A. Ahrabian, and D. P. Mandic, "Classification of motor imagery BCI using multivariate empirical mode decomposition," *IEEE Transactions on Neural Systems and Rehabilitation Engineering*, vol. 21, no. 1, pp. 10–22, 2013, doi: 10.1109/TNSRE.2012.2229296.

[4] "location over the motor cortex region of brain".

[5] K. W. Ha and J. W. Jeong, "Motor imagery EEG classification using capsule networks," *Sensors (Switzerland)*, vol. 19, no. 13, Jul. 2019, doi: 10.3390/s19132854.

[6] H. K. Lee and Y. S. Choi, "Application of continuous wavelet transform and convolutional neural network in decoding motor imagery brain-computer Interface," *Entropy*, vol. 21, no. 12, Dec. 2019, doi: 10.3390/e21121199.

[7] X. Zhao, H. Zhang, G. Zhu, F. You, S. Kuang, and L. Sun, "A Multi-Branch 3D Convolutional Neural Network for EEG-Based Motor Imagery Classification," *IEEE Transactions on Neural Systems and Rehabilitation Engineering*, vol. 27, no. 10, pp. 2164–2177, Oct. 2019, doi: 10.1109/TNSRE.2019.2938295.

[8] R. Alazrai, M. Abuhijleh, H. Alwanni, and M. I. Daoud, "A Deep Learning Framework for Decoding Motor Imagery Tasks of the Same Hand Using EEG Signals," *IEEE Access*, vol. 7, pp. 109612–109627, 2019, doi: 10.1109/ACCESS.2019.2934018.

[9] S. Chaudhary, S. Taran, V. Bajaj, and A. Sengur, "Convolutional Neural Network Based Approach Towards Motor Imagery Tasks EEG Signals Classification," *IEEE Sens J*, vol. 19, no. 12, pp. 4494–4500, Jun. 2019, doi: 10.1109/JSEN.2019.2899645.

[10] P. Thodoroff, J. Pineau, and A. Lim, "Learning Robust Features using Deep Learning for Automatic Seizure Detection." [Online]. Available: http://www.bhutanbrain.com

[11] J.-H. Cho, J.-H. Jeong, K.-H. Shim, D.-J. Kim, and S.-W. Lee, "Classification of Hand Motions within EEG Signals for Non-Invasive BCI-Based Robot Hand Control," in *2018 IEEE International Conference on Systems, Man, and Cybernetics (SMC)*, Oct. 2018, pp. 515–518. doi: 10.1109/SMC.2018.00097.

[12] V. Mishuhina and X. Jiang, "Feature Weighting and Regularization of Common Spatial Patterns in EEG-Based Motor Imagery BCI," *IEEE Signal Process Lett*, vol. 25, no. 6, pp. 783–787, Jun. 2018, doi: 10.1109/LSP.2018.2823683.

[13] B. Kanuparthi, A. C. Turlapaty, and B. Gokaraju, "An Ensemble Approach for Classification of Reach and Grasp Movements based on EEG Signals," in *Proceedings - Applied Imagery Pattern Recognition Workshop*, 2021, vol. 2021-October. doi: 10.1109/AIPR52630.2021.9762070.

[14] A. Altameem, J. Singh Sachdev, V. Singh, R. Chandra Poonia, S. Kumar, and A. Khader Jilani Saudagar, "Performance Analysis of Machine Learning Algorithms for Classifying Hand Motion-Based EEG Brain Signals," *Computer Systems Science and Engineering*, vol. 42, no. 3, pp. 1095–1107, 2022, doi: 10.32604/csse.2022.023256.

[15] C. Ieracitano, F. C. Morabito, A. Hussain, and N. Mammone, "A Hybrid-Domain Deep Learning-Based BCI For Discriminating Hand Motion Planning From EEG Sources," *Int J Neural Syst*, vol. 31, no. 09, p. 2150038, Sep. 2021, doi: 10.1142/S0129065721500386.

[16] H. Li, M. Ding, R. Zhang, and C. Xiu, "Motor imagery EEG classification algorithm based on CNN-LSTM feature fusion network," *Biomed Signal Process Control*, vol. 72, p. 103342, Feb. 2022, doi: 10.1016/j.bspc.2021.103342.

[17] N. T. M. Huong, H. Q. Linh, and L. Q. Khai, "Classification of Left/Right Hand Movement EEG Signals Using Event Related Potentials and Advanced Features," in *6th International Conference on the Development of Biomedical Engineering in Vietnam (BME6)*, 2018, pp. 209–215. doi: 10.1007/978-981-10-4361-1_35.

[18] M. Jochumsen and I. K. Niazi, "Detection and classification of single-trial movement-related cortical potentials associated with functional lower limb movements," *J Neural Eng*, vol. 17, no. 3, p. 35009, Jul. 2020, doi: 10.1088/1741-2552/ab9a99.

[19] M. Mohseni, V. Shalchyan, M. Jochumsen, and I. K. Niazi, "Upper limb complex movements decoding from pre-movement EEG signals using wavelet common spatial patterns," *Comput Methods Programs Biomed*, vol. 183, p. 105076, Jan. 2020, doi: 10.1016/j.cmpb.2019.105076.

[20] X. Yong and C. Menon, “EEG Classification of Different Imaginary Movements within the Same Limb,” *PLoS One*, vol. 10, no. 4, p. e0121896, Apr. 2015, doi: 10.1371/journal.pone.0121896.
[21] Y. Jiang, C. Chen, X. Zhang, W. Zhou, C. Chen, and S. Lemos, “EEG-Based Hand Motion Pattern Recognition Using Deep Learning Network Algorithms,” in *Proceedings of the 2020 9th International Conference on Computing and Pattern Recognition*, Jan. 2021, pp. 73–79. doi: 10.1145/3436369.3437433.
[22] G. Lange, C. Y. Low, K. Johar, F. A. Hanapiah, and F. Kamaruzaman, “Classification of Electroencephalogram Data from Hand Grasp and Release Movements for BCI Controlled Prosthesis,” *Procedia Technology*, vol. 26, pp. 374–381, Jan. 2016, doi: 10.1016/j.protcy.2016.08.048.
[23] S. C. Lin, D. Gervasoni, and M. A. L. Nicolelis, “Fast modulation of prefrontal cortex activity by basal forebrain noncholinergic neuronal ensembles,” *J Neurophysiol*, vol. 96, no. 6, pp. 3209–3219, Dec. 2006, doi: 10.1152/jn.00524.2006.
[24] R. T. Schirrmeister *et al.*, “Deep learning with convolutional neural networks for EEG decoding and visualization,” *Hum Brain Mapp*, vol. 38, no. 11, pp. 5391–5420, Nov. 2017, doi: 10.1002/hbm.23730.
[25] S. Sakhavi, C. Guan, and S. Yan, “Learning Temporal Information for Brain-Computer Interface Using Convolutional Neural Networks,” *IEEE Trans Neural Netw Learn Syst*, vol. 29, no. 11, pp. 5619–5629, Nov. 2018, doi: 10.1109/TNNLS.2018.2789927.
[26] “Anatomy_for_the_Medical_Clinician”.
[27] “PARTS OF BRAIN AND THEIR FUNCTIONS-CLASS 10 BIOLOGY-CHAPTER 7-CONTROL AND CO-ORDINATION-DETAILED EXPLANATION □ □ □ □,” 2022. [Online]. Available: https://edugyanshala.com/parts-of-brain-and-their-functions-class-10-biology-chapter-7-control-and-co-ordination-detailed-explanation/
[28] J. Knierim, “Section 3: Motor Systems Chapter 5: Cerebellum.” [Online]. Available: https://nba.uth.tmc.edu/neuroscience/m/s3/chapter05.html
[29] “Lobes of the brain.” Dec. 2016. [Online]. Available: https://qbi.uq.edu.au/brain/brain-anatomy/lobes-brain
[30] “Pons,” *Wikipedia*. Jul. 2022. [Online]. Available: https://en.wikipedia.org/w/index.php?title=Pons&oldid=1100340652
[31] S. Herculano-Houzel, “The human brain in numbers: A linearly scaled-up primate brain,” *Frontiers in Human Neuroscience*, vol. 3, no. NOV. Frontiers Media S. A., Nov. 09, 2009. doi: 10.3389/neuro.09.031.2009.
[32] “BOOK-BIOLOGY FOR MAJORS II (LUMEN).” [Online]. Available: https://LibreTexts.org
[33] “substances interact with the neurological system”.
[34] F. L. da Silva, “EEG: Origin and measurement,” in *EEG - fMRI: Physiological Basis, Technique, and Applications*, Springer Berlin Heidelberg, 2010, pp. 19–38. doi: 10.1007/978-3-540-87919-0_2.
[35] “Dipole,” *Wikipedia*. Jun. 2022. [Online]. Available: https://en.wikipedia.org/w/index.php?title=Dipole&oldid=1093645311
[36] L. R. Hochberg *et al.*, “Neuronal ensemble control of prosthetic devices by a human with tetraplegia,” *Nature*, vol. 442, no. 7099, pp. 164–171, Jul. 2006, doi: 10.1038/nature04970.
[37] J. R. Wolpaw and D. J. Mcfarland, “Control of a two-dimensional movement signal by a noninvasive brain-computer interface in humans,” 2004. [Online]. Available: www.pnas.orgcgidoi10.1073pnas.0403504101
[38] L. Haas, “Hans Berger (1873–1941), Richard Caton (1842–1926), and electroencephalography,” *J Neurol Neurosurg Psychiatry*, vol. 74, no. 1, p. 9, Jan. 2003, doi: 10.1136/jnnp.74.1.9.
[39] F. Popescu, S. Fazli, Y. Badower, B. Blankertz, and K. R. Müller, “Single trial classification of motor imagination using 6 dry EEG electrodes,” *PLoS One*, vol. 2, no. 7, Jul. 2007, doi: 10.1371/journal.pone.0000637.
[40] Lawrence. Rowe, ACM Special Interest Group on Multimedia., Association for Computing Machinery. Special Interest Group on Data Communications., SIGGRAPH., and ACM Digital Library., *Proceedings of the tenth ACM International Conference on Multimedia : Juan-les-Pins, December 01-06, 2002*. Association for Computing Machinery, 2004.
[41] M. Okamoto *et al.*, “Three-dimensional probabilistic anatomical cranio-cerebral correlation via the international 10-20 system oriented for transcranial functional brain mapping,” *Neuroimage*, vol. 21, no. 1, pp. 99–111, Jan. 2004, doi: 10.1016/j.neuroimage.2003.08.026.
[42] “User Tutorial:EEG Measurement Setup - BCI2000 Wiki.” [Online]. Available: https://www.bci2000.org/mediawiki/index.php/User_Tutorial:EEG_Measurement_Setup
[43] “English: EEG electrode positions in the 10-10 system using modified combinatorial nomenclature as presented by Klem, Lüders, Jasper, & Elger (1999). The electrode sites are colour-coded according to the lobes of the brain which their labels (F, C, P, O, and T) represent. The head indicates the location of the

fiducials: the nasion, the (left) pre-auricular point, and the inion. The font used for the electrode labels is Iosevka Medium." Nov. 2020. [Online]. Available: https://commons.wikimedia.org/wiki/File:EEG_10-10_system_with_additional_information.svg
[44] M. A. Lebedev and M. A. L. Nicolelis, "Brain-machine interfaces: past, present and future," *Trends Neurosci*, vol. 29, no. 9, pp. 536–546, Sep. 2006, doi: 10.1016/j.tins.2006.07.004.
[45] J. R. Wolpaw, N. Birbaumer, D. J. McFarland, G. Pfurtscheller, and T. M. Vaughan, "Brain-computer interfaces for communication and control," *Clin Neurophysiol*, vol. 113, no. 6, pp. 767–791, Jun. 2002, doi: 10.1016/s1388-2457(02)00057-3.
[46] T. M. Vaughan *et al.*, "Brain-computer interface technology: a review of the Second International Meeting," *IEEE Trans Neural Syst Rehabil Eng*, vol. 11, no. 2, pp. 94–109, Jun. 2003, doi: 10.1109/tnsre.2003.814799.
[47] D. McMullen *et al.*, "Demonstration of a Semi-Autonomous Hybrid Brain–Machine Interface Using Human Intracranial EEG, Eye Tracking, and Computer Vision to Control a Robotic Upper Limb Prosthetic," *IEEE Transactions on Neural Systems and Rehabilitation Engineering*, 2014, doi: 10.1109/TNSRE.2013.2294685.
[48] B. Z. Allison, E. W. Wolpaw, and J. R. Wolpaw, "Brain-computer interface systems: progress and prospects," *Expert Rev Med Devices*, vol. 4, no. 4, pp. 463–474, Jul. 2007, doi: 10.1586/17434440.4.4.463.
[49] M. E. J. Kouijzer, J. M. H. de Moor, B. J. L. Gerrits, J. K. Buitelaar, and H. T. van Schie, "Long-term effects of neurofeedback treatment in autism," *Res Autism Spectr Disord*, vol. 3, no. 2, pp. 496–501, Apr. 2009, doi: 10.1016/j.rasd.2008.10.003.
[50] S. G. Mason and G. E. Birch, "A general framework for brain-computer interface design," *IEEE Trans Neural Syst Rehabil Eng*, vol. 11, no. 1, pp. 70–85, Mar. 2003, doi: 10.1109/TNSRE.2003.810426.
[51] "BCI Competition III." [Online]. Available: https://www.bbci.de/competition/iii/
[52] G. E. Hinton and R. R. Salakhutdinov, "Reducing the Dimensionality of Data with Neural Networks," *Science (1979)*, vol. 313, no. 5786, pp. 504–507, Jul. 2006, doi: 10.1126/science.1127647.
[53] Y. Lecun, L. Bottou, Y. Bengio, and P. Haffner, "Gradient-based learning applied to document recognition," *Proceedings of the IEEE*, vol. 86, no. 11, pp. 2278–2324, Nov. 1998, doi: 10.1109/5.726791.
[54] A. Krizhevsky, I. Sutskever, and G. E. Hinton, "ImageNet Classification with Deep Convolutional Neural Networks," in *Advances in Neural Information Processing Systems*, 2012, vol. 25. [Online]. Available: https://papers.nips.cc/paper/2012/hash/c399862d3b9d6b76c8436e924a68c45b-Abstract.html
[55] Z. Jiang and S. Gao, "An intelligent recommendation approach for online advertising based on hybrid deep neural network and parallel computing," *Cluster Comput*, vol. 23, no. 3, pp. 1987–2000, Sep. 2020, doi: 10.1007/s10586-019-02959-5.
[56] K. Simonyan and A. Zisserman, "Very Deep Convolutional Networks for Large-Scale Image Recognition." arXiv, Apr. 2015. doi: 10.48550/arXiv.1409.1556.
[57] C. Ostertag, "The Shortest Introduction To Deep Learning You Will Find On The Web," *Analytics Vidhya*. Oct. 2019. [Online]. Available: https://medium.com/analytics-vidhya/the-shortest-introduction-to-deep-learning-you-will-find-on-the-web-25a9975bbe1d
[58] "Medium," *Medium*. [Online]. Available: https://towardsdatascience.com/a-gentle-introduction-to-machine-learning-599210ec34ad?gi=4edd97c93144
[59] "Deep Learning with Python," *Manning Publications*. [Online]. Available: https://www.manning.com/books/deep-learning-with-python
[60] S. H. Kim, Z. W. Geem, and G. T. Han, "Hyperparameter optimization method based on harmony search algorithm to improve performance of 1D CNN human respiration pattern recognition system," *Sensors (Switzerland)*, vol. 20, no. 13, pp. 1–20, Jul. 2020, doi: 10.3390/s20133697.
[61] A. Azarfar, N. Calcini, C. Huang, F. Zeldenrust, and T. Celikel, "Neural coding: A single neuron's perspective," *Neurosci Biobehav Rev*, vol. 94, pp. 238–247, Nov. 2018, doi: 10.1016/j.neubiorev.2018.09.007.
[62] J. R. Laurence and C. Perry, "Hypnotically created memory among highly hypnotizable subjects," *Science*, vol. 222, no. 4623, pp. 523–524, Nov. 1983, doi: 10.1126/science.6623094.
[63] "BNCI Horizon 2020," *BNCI Horizon 2020*.
[64] R. Oostenveld and P. Praamstra, "The ®ve percent electrode system for high-resolution EEG and ERP measurements." [Online]. Available: www.elsevier.com/locate/clinph
[65] C. Breitwieser, A. Kreilinger, and C. Neuper, "The TOBI Hybrid BCI-The Data Acquisition Module." [Online]. Available: https://www.researchgate.net/publication/267801490
[66] A. Schwarz, C. Escolano, L. Montesano, and G. R. Müller-Putz, "Analyzing and Decoding Natural Reach-and-Grasp Actions Using Gel, Water and Dry EEG Systems," *Front Neurosci*, vol. 14, Aug. 2020, doi: 10.3389/fnins.2020.00849.

[67] A. Schwarz, J. Pereira, R. Kobler, and G. R. Müller−putz, “Unimanual and Bimanual Reach-and-Grasp Actions Can Be Decoded From Human EEG,” 2019.
[68] S. Tsuchimoto *et al.*, “Use of common average reference and large-Laplacian spatial-filters enhances EEG signal-to-noise ratios in intrinsic sensorimotor activity,” *J Neurosci Methods*, vol. 353, p. 109089, Apr. 2021, doi: 10.1016/j.jneumeth.2021.109089.
[69] “Electric_Fields_of_the_Brain”.
[70] “An Introduction to the Event-Related Potential Technique,” *MIT Press*. [Online]. Available: https://mitpress.mit.edu/9780262525855/an-introduction-to-the-event-related-potential-technique/
[71] L. Deecke, “Planning, preparation, execution, and imagery of volitional action,” *Cognitive Brain Research*, vol. 3, no. 2, pp. 59–64, Mar. 1996, doi: 10.1016/0926-6410(95)00046-1.
[72] N. Birbaumer, T. Elbert, A. G. Canavan, and B. Rockstroh, “Slow potentials of the cerebral cortex and behavior,” *Physiol Rev*, vol. 70, no. 1, pp. 1–41, Jan. 1990, doi: 10.1152/physrev.1990.70.1.1.
[73] H. Shibasaki and M. Hallett, “What is the Bereitschaftspotential?,” *Clin Neurophysiol*, vol. 117, no. 11, pp. 2341–2356, Nov. 2006, doi: 10.1016/j.clinph.2006.04.025.
[74] W. Lang, R. Beisteiner, G. Lindinger, and L. Deecke, “Changes of cortical activity when executing learned motor sequences,” *Exp Brain Res*, vol. 89, no. 2, pp. 435–440, May 1992, doi: 10.1007/BF00228259.
[75] I. M. Tarkka and M. Hallett, “Cortical topography of premotor and motor potentials preceding self-paced, voluntary movement of dominant and non-dominant hands,” *Electroencephalogr Clin Neurophysiol*, vol. 75, no. 1, pp. 36–43, Feb. 1990, doi: 10.1016/0013-4694(90)90150-I.
[76] D. JIANG, Y. nan LU, Y. MA, and Y. WANG, “Robust sleep stage classification with single-channel EEG signals using multimodal decomposition and HMM-based refinement,” *Expert Syst Appl*, vol. 121, pp. 188–203, May 2019, doi: 10.1016/j.eswa.2018.12.023.
[77] N. Michielli, U. R. Acharya, and F. Molinari, “Cascaded LSTM recurrent neural network for automated sleep stage classification using single-channel EEG signals,” *Comput Biol Med*, vol. 106, pp. 71–81, Mar. 2019, doi: 10.1016/j.compbiomed.2019.01.013.
[78] “10607082”.
[79] P. Bhuvaneswari, “International Journal of Computer Applications (0975 – 8887) Volume 63– No.13, February 2013 Support Vector Machine Technique for EEG Signals,” *International Journal of Computer Applications (0975 – 8887)*, vol. 63, pp. 1–5, Oct. 2013.
[80] S. Singh, “ELU as an Activation Function in Neural Networks .,” *Deep Learning University*. Jun. 2020. [Online]. Available: https://deeplearninguniversity.com/elu-as-an-activation-function-in-neural-networks/
[81] D. P. Kingma and J. Ba, “Adam: A Method for Stochastic Optimization,” Dec. 2014, [Online]. Available: http://arxiv.org/abs/1412.6980
[82] R. T. Schirrmeister *et al.*, “Deep learning with convolutional neural networks for EEG decoding and visualization,” *Hum Brain Mapp*, vol. 38, no. 11, pp. 5391–5420, Nov. 2017, doi: 10.1002/hbm.23730.
[83] I. Freeman, L. Roese-Koerner, and A. Kummert, “EffNet: An Efficient Structure for Convolutional Neural Networks,” Jan. 2018, [Online]. Available: http://arxiv.org/abs/1801.06434